universe

MDPI

Article

A Scale Invariant Fully Conformal Cosmological Model and Its Support by Astrophysical Data †

Richard Dvorsky

Faculty of Materials Science and Technology, Centre for Advanced Innovation Technologies, VSB—Technical University of Ostrava, 17. Listopadu 15/2172, 708 00 Ostrava, Czech Republic; richard.dvorsky@vsb.cz

† This work is a new modified and extended version of a preprint: Dvorsky, Richard, A Simple Fully Conformal Solution of Einstein's Gravitational Equations and the Agreement of its Implications with Astrophysical Data (1 March 2023) on the preprint server SSRN. Available at SSRN: https://ssrn.com/abstract=4373727 or http://dx.doi.org/10.2139/ssrn.4373727 from (1 March 2023).

Abstract: According to general relativity, the cosmological redshift may be caused by other mechanisms than the source moving away from the observer. It can occur on a global scale, similar to the gravitational redshift near massive stars. In principle, these are differences in the time-dependent global metric field between the source in the past and the observer in the present. In this paper we attempt a new interpretation of the simple solution of Einstein's equations within a fully conformal metric for the case of a time-independent energy-momentum tensor. The scaling factor here acts identically on all four space-time coordinates and the speed of light is independent of the conformal time. The fully conformal metric is interpreted here as a universal geometric background which is scale invariant and acts universally on all objects, including gauges and clocks, regardless of their dimensions and internal interactions. The associated scale invariant exponential expansion is thus only relative and all observers at different times are completely equal. The model introduces the concept of the appearent age of the universe, which is the limiting consequence of time dilation into the past, and corresponds to the present value of the age of the universe H^{-1} according to the standard model. This appearent age is the same for all observers, and the Hubble constant is thus a true universal constant, invariant to time translations. The motivation of this work was to test the possibility of the above cosmological redshift mechanism in confrontation with astrophysical data. Probably the most important consequence is the generalized formulation and interpretation of the Hubble-Lemaître law $z(r) = (e^{Hr/c} - 1)$, which shows good agreement with astrophysical data even for the most distant supernovae. Confronting the conformal metric model with some astrophysical data shows an interesting agreement with the observed spatial distribution of astrophysical sources such as γ-ray bursts and quasars. On a cosmological scale, the above fully conformal metric naturally determines the global energy density, spatial flatness, and solves the horizon problem and Olbers' paradox in infinite spacetime.

Keywords: conformal metric; scale invariancy; cosmologhical redshift; gamma burst; quasars; spatial flatness; critical density; Olbers' paradox

Academic Editors: Emmanuel N. Saridakis and Panayiotis Stavrinos

Received: 23 November 2024
Revised: 28 December 2024
Accepted: 7 January 2025
Published: 21 January 2025

Citation: Dvorsky, R. A Scale Invariant Fully Conformal Cosmological Model and Its Support by Astrophysical Data. *Universe* **2025**, *11*, 30. https://doi.org/10.3390/universe11020030

1. Introduction

According to the standard model, the currently accepted explanation for the cosmological redshift is a real spatial expansion of the universe with an origin in the Big Bang. However, could the cosmological redshift also be interpreted as the result of a difference

between the global metric field around a radiating astrophysical source in the past and the global metric field around an observer in the present?

Astrophysical data for the cosmological redshift are in most cases already published in the form of a dependence of the source receding rate on the distance from the observer. This transformation of real experimental data into terms of the preferred standard cosmological model may be misleading for the further development of the field. The above question about an alternative interpretation of the cosmological redshift was raised in the past by Fritz Zwicky [1]. However, his concept of "tired light" corresponded to a gravitational redshift based on local curvatures of spacetime by the masses of galaxies, and the redshift effect depended on local spatial distances from galactic centres. This created a problem with observational data showing a global dependence of redshift on distance from any observer.

In this paper we attempt to interpret the cosmological redshift based on the aforementioned differences in the global metric field between the two time levels in spacetime. This interpretation should correspond to a global solution of Einstein's gravitational equations whose metric field varies with time $g_{\mu\nu} = g_{\mu\nu}(t)$, while at the same time ensuring full covariance of the laws of nature at every time of the space-time continuum. One of the simplest solutions that satisfies the above requirements is a flat, fully conformal Minkowski metric with time scaling $g_{\mu\nu}(t) = \psi(t) \cdot \eta_{\mu\nu}$, $g_{\mu\nu}(0) = \eta_{\mu\nu}$, where the time distance of the source t is measured into the past from the zero point $r = 0$ of the origin of the observer's coordinates. When the source radiation is observed at a distance $r = ct$ from the observer, we obtain redshift generally defined as $z = \sqrt{g_{44}(r)/g_{44}(0)} - 1 = \sqrt{g_{44}(t)/g_{44}(0)} - 1$. In this article, the aforementioned metric is derived on the basis of the a priori presumption of time-independent energy-momentum tensor and requirements of full conformity of all space-time coordinates due to acceptance of "perfect cosmological principle" [2,3]. Its physical meaning is then analysed in confrontation not only with cosmological redshift data, but also with some other astrophysical data.

The approach used in this work rests in the finding of the solution of Einstein gravity equations in the form of the fully conformal metric, where natural physical time t has a conformal character and the scaling factor acts equivalently on all space-time coordinates. In the case of such solutions, the covariant form of Maxwell's equations is preserved and the speed of light does not change over time (c = const.), which can be considered a positive property and a simplification within the respective models. However, the primary aim of this paper is not to derive a specific form of the fully conformal Minkowski metric per se, but a deeper analysis of its physical content assuming time-independent energy-momentum tensor and the analysis of its possibility to describe astrophysical observational data.

For the various variants of energy-momentum tensors in current cosmological models, most solutions of Einstein's gravitational equations are found in the assumed form of the FLRW metric with linear physical parameter of cosmological time t and scaling factor $a(t)$ acting only on space coordinates. By the establishment of FLRW-conformal time $d\eta = dt/a(t)$ it is possible these solutions transform into the formally identical mathematical form of fully conformal metric.

In the field of conformal solutions of Einstein's gravitational equations, a number of mostly theoretical papers have been published [4–10] including conformal forms of the well-known Lamaitre-Friedman-Robertson-Walker (FLRW) metric [11–14]. In these FLRW metrics, the Weyl conformal tensor disappears [15], which in most of these works allowed to achieve full space-time conformality by a suitable transformation of the space-time coordinates. A comprehensive survey of these secondary conformal forms of the primary FLRW metric has been summarised by Ibison [16].

It may seem that the whole message of this work can be "solved by naming and tagging" and completely identifying the fully conformal metric, with "FLRW-conformal metric", which was derived from FLRW by a transformation—therefore "nothing new". However, is this derived "FLRW-conformal metric" physically identical with above mentioned "the fully conformal metric", which was analyzed in this article? A general calculation shows, that both mentioned conformal metrics are not completely identical. The corresponding Friedmann equations for a flat space without a cosmological term show a different structure and the corresponding equations of state will also differ.

The fully conformal global metric with a time scaling is derived based on four premises:

PREMISE 1: Extrapolation of Einstein's gravitational equations [17] to a global cosmological scale is the correct description of the geometry of the physical universe.

PREMISE 2: The space-time structure of the universe is homogeneous and its spatial part is isotropic ("perfect cosmological principle" applies [2,3]), and the average spatial distribution of astrophysical objects does not vary on global cosmological scales.

PREMISE 3: The local reference observer system has a Minkowski metric: $g_{\mu\nu} \rightarrow \eta_{\mu\nu}$.

PREMISE 4: The global metric field acts universally on all units of length and time scales, independent of how they are dimensioned and materialised.

Although references [2,3], refer to the steady-state theory of the expanding universe, this paper differs significantly from that concept. Unlike these papers, the solution of Einstein's gravitational equations is sought here in the form of a fully conformal metric and not the Robertson-Walker metric. The fully conformal metric is interpreted in this paper as a universal geometric background, that affects all objects, including gauges and clocks, regardless of their dimensions and internal coupling interactions. As a consequence of this interpretation, the associated expansion is only relative and all observers at different times are completely equal. In this paper, the implications of the fully conformal metric are confronted with astrophysical data such as cosmological redshift and the observable spatial distribution of quasars and γ-ray bursts. On a cosmological scale, the fully conformal metric naturally determines energy density and spatial flatness, and solves the horizon problem and Olbers' paradox in infinite spacetime.

2. Fully Conformal Spacetime with Time Scaling

Let the coordinates' origin of the local inertial system (observer location), in which the microwave background of the universe is isotropic, be our "central observer point" (in next text COP). It can be located at any place and time (for simplicity let us accept the condition of local absence of gravitational bodies). Taking into account the experimentally confirmed spatial flatness in the vicinity of the COP, we establish Minkowski coordinates $x_o = (x_{o1}, x_{o2}, x_{o3}, x_{o4} = ct_o)$ with own time t_o for this local inertial system with the origin just at the COP. Since the real universe allows for an infinite number of alternative COPs, for the following analysis we restrict ourselves to a single COP at the origin of the above local Minkowski coordinate system $\boldsymbol{x_o} = (x_{o1}, x_{o2}, x_{o3}, x_{o4} = ct_o)$. This local Minkowski coordinate system near the origin merges with the general curvilinear global coordinate systém $\boldsymbol{x} = (x_1, x_2, x_3, x_4 = ct)$, which is used to locate points on a whole variety of the corresponding spacetime, and which parametrizes its global metric field $g_{\mu\nu}(\boldsymbol{x})$. All further considerations are based on PREMISE 1, PREMISE 2 and PREMISE 3 above.

Let us find solutions of Einstein's gravitational equations without a cosmological constant in the form of a fully conformal Minkowski metric $\eta_{\mu\nu}$ with purely temporal global scaling $\psi(x_4)$

$$R_{\mu\nu} - \frac{1}{2}Rg_{\mu\nu} = \kappa T_{\mu\nu} \cdots \begin{cases} g_{\mu\nu}(x_4) \stackrel{\text{def}}{=} \psi(x_4)\eta_{\mu\nu} = \psi(x_4)\begin{pmatrix} 1 & 0 & 0 & 0 \\ 0 & 1 & 0 & 0 \\ 0 & 0 & 1 & 0 \\ 0 & 0 & 0 & -1 \end{pmatrix} \\ ds^2 = g_{\mu\nu}(x_4)dx_\mu dx_\nu = \psi(x_4)\left(dx_1^2 + dx_2^2 + dx_3^2 - dx_4^2\right) \end{cases} \tag{1}$$

From the corresponding Christoffel symbols $\Gamma^{\mu}{}_{\nu\lambda}$ as functions of single time variable x_4, only the following functions are nonzero for the conformal metric tensor (1) Appendix A:

$$\Gamma^{\mu}{}_{\nu\lambda}(x_4) = \tfrac{1}{2}g^{\mu\alpha}(x_4)(\partial_\nu g_{\alpha\lambda}(x_4) + \partial_\lambda g_{\alpha\nu}(x_4) - \partial_\alpha g_{\nu\lambda}(x_4))$$

$$\left.\begin{aligned} \Gamma^1{}_{14}(x_4) &= \Gamma^1{}_{41}(x_4) \\ \Gamma^2{}_{24}(x_4) &= \Gamma^2{}_{42}(x_4) \\ \Gamma^3{}_{34}(x_4) &= \Gamma^3{}_{43}(x_4) \\ \Gamma^4{}_{11}(x_4) = \Gamma^4{}_{22}(x_4) &= \Gamma^4{}_{33}(x_4) = \Gamma^4{}_{44}(x_4) \end{aligned}\right\} = \tfrac{1}{2}\partial_4 \ln\psi(x_4) \quad . \tag{2}$$

The following Ricci tensor is non-zero only in the diagonal components, and the scalar curvature R is also a non-zero function of single time variable x_4 Appendix C.

$$\begin{aligned} &R_{11} = R_{22} = R_{33} = \tfrac{1}{2}\partial_4^2 \ln\psi(x_4) + \tfrac{1}{2}(\partial_4 \ln\psi(x_4))^2 \\ &R_{44} = -\tfrac{3}{2}\partial_4^2 \ln\psi(x_4) \\ &R = \left(-3\partial_4^2 \ln\psi(x_4) - \tfrac{3}{2}(\partial_4 \ln\psi(x_4))^2\right)\psi^{-1}(x_4) \end{aligned} \quad . \tag{3}$$

While the purely spatial part of the 3D has the character of a flat space E3 [18], the total global curvature R of the spacetime according to (1) is generally non-zero.

In a uniform (homogeneous and spacial isotropic) universe, the energy-momentum tensor $T_{\mu\nu}$ on a global cosmological scale can be approximated by a model of inert incoherent dust (particulate matter) with energy density ε_p uniformly dispersed in an ideal static space-time fluid with energy density ε_s and global pressure p. With respect to PREMISE 2, all the parameters mentioned are independent of time.

$$T_{\mu\nu} = \underbrace{\begin{pmatrix} 0 & 0 & 0 & 0 \\ 0 & 0 & 0 & 0 \\ 0 & 0 & 0 & 0 \\ 0 & 0 & 0 & \varepsilon_p \end{pmatrix}}_{T^{par}{}_{\mu\nu}} + \underbrace{\begin{pmatrix} p & 0 & 0 & 0 \\ 0 & p & 0 & 0 \\ 0 & 0 & p & 0 \\ 0 & 0 & 0 & \varepsilon_s \end{pmatrix}}_{T^{spa}{}_{\mu\nu}} \rightarrow T_{\mu\nu} = \begin{pmatrix} p & 0 & 0 & 0 \\ 0 & p & 0 & 0 \\ 0 & 0 & p & 0 \\ 0 & 0 & 0 & (\varepsilon_p + \varepsilon_s) \end{pmatrix}. \tag{4}$$

While the $T^{par}{}_{\mu\nu}$ tensor corresponds to localised particulate forms of energy, such as gases, dust and stars, the $T^{spa}{}_{\mu\nu}$ tensor corresponds to the global energy structure of a continuous metric space-time field. After substituting the energy-momentum tensor (4) into (1), we obtain conditions for a currently unknown scaling function $\psi(x_4)$ Appendix D.

$$R_{\mu\nu} - \frac{1}{2}Rg_{\mu\nu} = \kappa T_{\mu\nu} \rightarrow \begin{cases} \left.\begin{aligned} R_{11} - \tfrac{1}{2}R\psi(x_4)\eta_{11} &= \kappa p \\ R_{22} - \tfrac{1}{2}R\psi(x_4)\eta_{22} &= \kappa p \\ R_{33} - \tfrac{1}{2}R\psi(x_4)\eta_{33} &= \kappa p \end{aligned}\right\} & \rightarrow -\partial_4^2[\ln\psi(x_4)] - \tfrac{1}{4}(\partial_4[\ln\psi(x_4)])^2 = \kappa p \ \text{(a)} \\ \left.\begin{aligned} R_{44} - \tfrac{1}{2}R\psi(x_4)\eta_{44} &= \kappa\varepsilon \end{aligned}\right\} & \rightarrow \tfrac{3}{4}(\partial_4[\ln\psi(x_4)])^2 = \kappa(\varepsilon_p + \varepsilon_s) \quad \text{(b)} \end{cases} . \tag{5}$$

The solution of Equation (5b) gives a general form of the scaling function $\psi(x_4)$

$$\psi_{\pm}(x_4) = \psi(0)e^{\pm x_4\sqrt{\frac{4}{3}\kappa(\varepsilon_p+\varepsilon_s)}}. \tag{6}$$

The problem of alternatives $\psi_{-}(x_4)$ and $\psi_{+}(x_4)$ of the scaling function (6) will be discussed below. With respect to PREMISE 3, the scaling function (6) becomes:

$$\psi(0) = 1 \;\rightarrow\; \psi_{\pm}(x_4) = e^{\pm x_4\sqrt{\frac{4}{3}\kappa(\varepsilon_p+\varepsilon_s)}}. \tag{7}$$

At this stage, the exponent contains an as yet unspecified total density of homogeneously distributed energy (ε_p + ε_s). The formulation of the scaling function (7) will be confronted with the present cosmological redshift data in the next section to provide a concrete form of the conformal metric tensor (1).

3. Cosmological Redshift

Let us analyse the relative time flow at different radial distances from the COP. The spacetime interval $ds(x)$ is a function of the four-vector $x(x_1, x_2, x_3, x_4)$ due to the generally varying metric tensor $g_{\mu\nu}(x)$. Similarly, the differentials of the proper Minkowski coordinates ($x_{o1}(x)$, $x_{o2}(x)$, $x_{o3}(x)$, $x_{o4}(x)$) of the local inertial systems around any point x of spacetime, are a function of the four-vector x

$$\begin{aligned} g_{\mu\nu}(x)dx_\mu dx_\nu &= ds(x)^2 = \eta_{\mu\nu}dx_{o\mu}(x)dx_{o\nu}(x) \\ ds(x)^2 &= \underbrace{g_{11}(x)dx_1^2}_{\eta_{11}dx_{o1}(x)^2} + \underbrace{g_{22}(x)dx_2^2}_{\eta_{22}dx_{o2}(x)^2} + \underbrace{g_{33}(x)dx_3^2}_{\eta_{33}dx_{o3}(x)^2} + \underbrace{g_{44}(x)dx_4^2}_{\eta_{44}dx_{o4}(x)^2} \end{aligned}. \tag{8}$$

If the chosen position of the COP in spacetime is denoted by $\boldsymbol{x}(0, 0, 0, 0) \equiv \mathbf{0}$, then the Minkowski coordinates ($x_{o1}(\mathbf{0})$, $x_{o2}(\mathbf{0})$, $x_{o3}(\mathbf{0})$, $x_{o4}(\mathbf{0})$) of the corresponding local inertial system in the conformal metric (1) according to (7), coincide with the geodetic coordinates (x_1, x_2, x_3, x_4) in the vicinity of $\mathbf{0}$ (which is consistent with the Minkowski metric of the surrounding spacetime, confirmed by experimental experience-3D-spatial flatness and a large region with negligible cosmological redshift)

$$ds(\mathbf{0})^2 = \underbrace{g_{11}(\mathbf{0})dx_1^2}_{\eta_{11}dx_{o1}(\mathbf{0})^2} + \underbrace{g_{22}(\mathbf{0})dx_2^2}_{\eta_{22}dx_{o2}(\mathbf{0})^2} + \underbrace{g_{33}(\mathbf{0})dx_3^2}_{\eta_{33}dx_{o3}(\mathbf{0})^2} + \underbrace{g_{44}(\mathbf{0})dx_4^2}_{\eta_{44}dx_{o4}(\mathbf{0})^2}. \tag{9}$$

There is a well-known formula for the own time flow τ in a point event ($dx_{\mathrm{i}} = 0$, i = 1,2,3) at the COP $\mathbf{0}$ at any point $\boldsymbol{x}$ in spacetime [15,19]

$$\left.\begin{aligned} \eta_{44}dx_{o4}(x)^2 &= g_{44}(x)dx_4^2 \\ \eta_{44}dx_{o4}(\mathbf{0})^2 &= g_{44}(\mathbf{0})dx_4^2 \end{aligned}\right\} \rightarrow dx_{o4}(x) = dx_{o4}(\mathbf{0})\sqrt{\frac{g_{44}(x)}{g_{44}(\mathbf{0})}} \rightarrow dt_o(x) = dt_o(\mathbf{0})\sqrt{\frac{g_{44}(x)}{g_{44}(\mathbf{0})}}. \tag{10}$$

Within the conformal metric (1), the (10) takes the form of

$$dt_o(x) = dt_o(\mathbf{0})\sqrt{\frac{\eta_{44}\psi(x_4)}{\eta_{44}}} \rightarrow dt_o(x_4) = dt_o(0)\sqrt{\psi(x_4)}. \tag{11}$$

As a result of the assumption of the conformal metric (1) and relation (7), the Equation (11) takes the form

$$dt_o(x_4) = dt_o(0)\sqrt{\psi_{\pm}(x_4)} = dt_o(0)e^{\pm x_4\sqrt{\frac{\kappa}{3}(\varepsilon_p+\varepsilon_s)}}. \tag{12}$$

The negative time coordinate $x_4 \leq 0$ of the past defines a radial "observation sphere with positive radius" r (13)with respect to the COP

$$\left.\begin{array}{r} dr^2 = dx_1^2 + dx_2^2 + dx_3^2 \\ ds(x_4)^2 = 0 \end{array}\right\} \rightarrow \psi(x_4)dr^2 - \psi(x_4)dx_4^2 = 0 \rightarrow dr = -dx_4 \rightarrow r = -x_4. \quad (13)$$

If two different points emit light from a source with the same frequency $\nu(0)$, then we measure an identical value of $\nu(0) \sim 1/dt_o(0)$ for a source at $r = 0$ near the COP, while for a source at a large distance r the measured frequency $\nu(r) \sim 1/dt_o(r)$ will theoretically be higher or lower depending on the polarity of the exponent in (12)

$$\nu(r) = \nu(0)e^{\mp r\sqrt{\frac{\kappa}{3}(\varepsilon_p + \varepsilon_s)}}. \quad (14)$$

At this stage, the polarity of the exponent (14) can be decided based on experimental experience. Since a positive sign would represent a blue cosmological shift, it is appropriate to see it as "non-physical" for now, but this does not exclude its possible meaning in the future. On the contrary, a red cosmological shift ($\nu(r) < \nu(0)$) has been clearly confirmed experimentally, and therefore we will currently accept only the negative sign

$$\nu(r) = \nu(0)e^{-r\sqrt{\frac{\kappa}{3}(\varepsilon_p + \varepsilon_s)}}. \quad (15)$$

Let's reformulate the (15) to the "redshift" Equation (16)

$$z \stackrel{\text{def}}{=} \frac{\nu(0) - \nu(r)}{\nu(r)} \rightarrow z = e^{r\sqrt{\frac{\kappa}{3}(\varepsilon_p + \varepsilon_s)}} - 1, \quad (16)$$

which converges into the familiar linear form for small values of the exponent (small distances r from the COP)

$$z = \left(e^{r\sqrt{\frac{\kappa}{3}(\varepsilon_p + \varepsilon_s)}} \approx r\sqrt{\frac{\kappa}{3}(\varepsilon_p + \varepsilon_s)} + 1\right) - 1 \rightarrow z = \left[\sqrt{\frac{\kappa}{3}(\varepsilon_p + \varepsilon_s)}\right] r. \quad (17)$$

Equation (17) is formally equivalent to a linear formulation of the standard Hubble–Lemaître law for small cosmological distances

$$z = \frac{H}{c}r. \quad (18)$$

Combining (17) and (18), we obtain a final form that allows us to directly calculate the equivalent inertial mass density of the universe ($\rho_p + \rho_s$). Its value corresponds to the critical density ρ_{crit} [20] for the flat space solution of the Friedmann model

$$\left.\begin{array}{l} \frac{H}{c} = \sqrt{\frac{\kappa}{3}(\varepsilon_p + \varepsilon_s)} \\ \kappa = \frac{8\pi G}{c^4} \end{array}\right\} \rightarrow \rho_p + \rho_s = \frac{3H^2}{8\pi G} = \rho_{\text{crit}} = 8 \times 10^{-27}\ \text{kg} \cdot \text{m}^{-3} \rightarrow \boxed{\nu(r) = \nu(0)e^{-\frac{H}{c}r}}. \quad (19)$$

Based on this match (19), the Equation (16) can be expressed as the final form of the generalized Hubble–Lemaître law

$$\boxed{z = e^{\frac{H}{c}r} - 1}. \quad (20)$$

Its nonlinear character is clearly visible only at large cosmological distances r (see Figure 1).

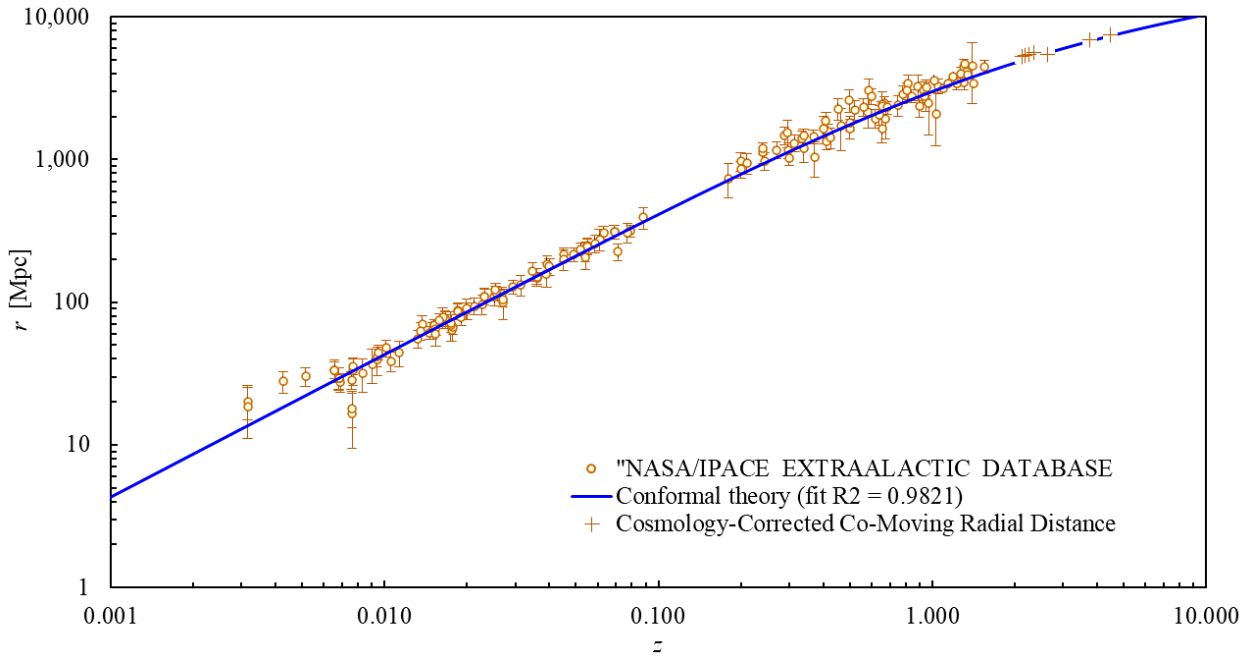

Figure 1. Hubble–Lemaître diagram: experimental points are taken from NASA/IPACE EXTRAGALACTIC DATABASE [21] and the blue curve—represents the fit of the generalized Hubble–Lemaître law (20) for a Hubble's parameter of 69.7 [km s^{-1}/Mpc] [22].

The coefficient of determination $R^2 = 0.9821$ in Figure 1 documents approximately a 98% fit of the model regression function (20) to the observational data and confirms the realistic nature of the mathematical formula of the generalized Hubble–Lemaître law (20). In this situation, it is worth pointing out that its nonlinearity is a direct consequence of the conformal solution of Einstein's gravitational Equation (1) without the cosmological term and it does not require the hypothetical concept of dark energy. Based on relations (17) and (18), the scaling function (7) and hence the metric tensor $g_{\mu\nu}$ takes a concrete form

$$\left.\begin{array}{l}\psi(x_4) = e^{x_4\sqrt{\frac{4}{3}\kappa(\varepsilon_p+\varepsilon_s)}} \\ \frac{H}{c} = \sqrt{\frac{\kappa}{3}(\varepsilon_p+\varepsilon_s)}\end{array}\right\} \rightarrow \psi(x_4) = e^{2\frac{H}{c}x_4} \rightarrow \boxed{g_{\mu\nu}(x_4) = e^{2\frac{H}{c}x_4}\eta_{\mu\nu}}, \left\{\begin{array}{c}\text{past}: x_4 < 0 \\ \text{COP}: x_4 = 0 \\ \text{future}: x_4 > 0\end{array}\right\} \quad (21)$$

The global spacetime determined by the metric tensor (21) is the fundamental geometry background of the universe on a cosmological scale. Due to the non-linear nature of Einstein's equations, the "composition" of local gravitational fields is not simply additive with the above cosmological background. For example, the flat Minkowski spacetime $\eta_{\mu\nu}$ can be replaced by a conformal metric (21) in the asymptotic limit of the Schwarzschild field for $r \rightarrow \infty$, but in the vicinity of a source of mass it is problematic to separate those two metric factors. This non-trivial situation is closely related to the still debated problem of whether cosmological expansion also occurs on a local scale in gravitationally bound systems.

4. Relativity of Observer Time and the Apparent Age of the Universe

Despite the formal similarity of the conformal metric factor to the e^{2Ht} expansion factor of the de Sitter solution [23], the factor (21) corresponds to different physical conditions than the de Sitter solution without particulate matter. With a non-zero fraction of particulate matter, it cannot be derived by simply introducing the standard conformal time into the FLRW metric for solving Einstein's equations (*the derived Friedmann equations are significantly different for the two cases*). The energy-momentum tensor contains a non-zero fraction of

particulate matter and the equations, on the other hand, do not contain the cosmological term that is the basis of de Sitter's solution.

Assuming global spacetime homogeneity and spatial isotropy of the universe (PREMISE 2), all COPs of such a spacetime must be completely equal, which corresponds to the "perfect cosmological principle" as formulated by Bondi, Gold and Hoyle in [2,3]. Here, however, two fundamental differences should be emphasized: in a scale invariant and fully conformal universe, expansion has only a relative observational character, similar to mass in special relativity, and the time-invariant global energy-momentum tensor does not require the continuous creation of new matter, unlike the familiar steady-state model.

The metric allows "linear extrapolation" of coordinates (x_1, x_2, x_3, x_4) from the vicinity of any COP to global Minkowski coordinates (x_{o1}, x_{o2}, x_{o3}, x_{o4}), so in the absence of gravitational field sources, the observer's local inertial frame in the COP is extended over the entire region of infinite spacetime

$$\left[\lim_{x_4\to 0} g_{\mu\nu}(x_4)dx_\mu dx_\nu = \eta_{\mu\nu}dx_\mu dx_\nu\right] = ds^2 = \left[\eta_{\mu\nu}dx_{o\mu}dx_{o\nu}\right] \tag{22}$$

and corresponds to the linear metric background used by Schwartschild as an asymptotic condition for the metric description of the central gravitational field. The 3D subspace (x_{o1}, x_{o2}, x_{o3}, x_{o4} = 0) then represents a "time slice of presence" starting at COP. Although the extrapolated coordinates (x_{o1}, x_{o2}, x_{o3}, x_{o4}) continuously cover the abstract Minkowski spacetime, they are not directly measurable from the COP due to the finite speed of light.

For directly measurable relative coordinates (x_1, x_2, x_3, x_4) with origin at any COP, we can set a term "observation coordinates". The transformation of differentials between the two types of coordinates is explicitly determined by the conformal metric and the extrapolation condition (22)

$$dx_{o\mu} = e^{\frac{H}{c}x_4}dx_\mu \tag{23}$$

which gives the quantitative ratio of spatiotemporal scales for two different time levels $x_4 = 0$ and $x_4 < 0$. Especially for the time coordinate x_4, we can derive the transformation formula ($x_4 \to x_{o4}$)$\leftrightarrow$($t \to t_o$) by integration

$$x_{o4} = \int_0^{x_4} e^{\frac{H}{c}x_4}dx_4 \;\to\; \begin{cases} x_{o4} = \dfrac{c}{H}\left(e^{\frac{H}{c}x_4} - 1\right) \to \boxed{t_o = \dfrac{1}{H}\left(e^{Ht} - 1\right)} \\ \min t_o = \dfrac{1}{H}\lim\limits_{t\to-\infty}\left(e^{Ht} - 1\right) = -\dfrac{1}{H} \approx -14\times 10^9 \text{ yr} \end{cases} . \tag{24}$$

The relationship between local and observation time is shown graphically in Figure 2 and their mutual deviation is at most 3.5% up to $t \approx -10^9$ years, but below values of $t \approx -14 \times 10^9$ yr (into the past), the deviation becomes larger, and the extreme dilation of the observational time t results in a limiting boundary of the apparent origin of the local time min t_o, which appears to be the "age of the universe".

As we go deeper into the past, the increasingly significant dilation of observational time causes real physical effects such as the redshift, which around this threshold time level gradually grows beyond all limits.

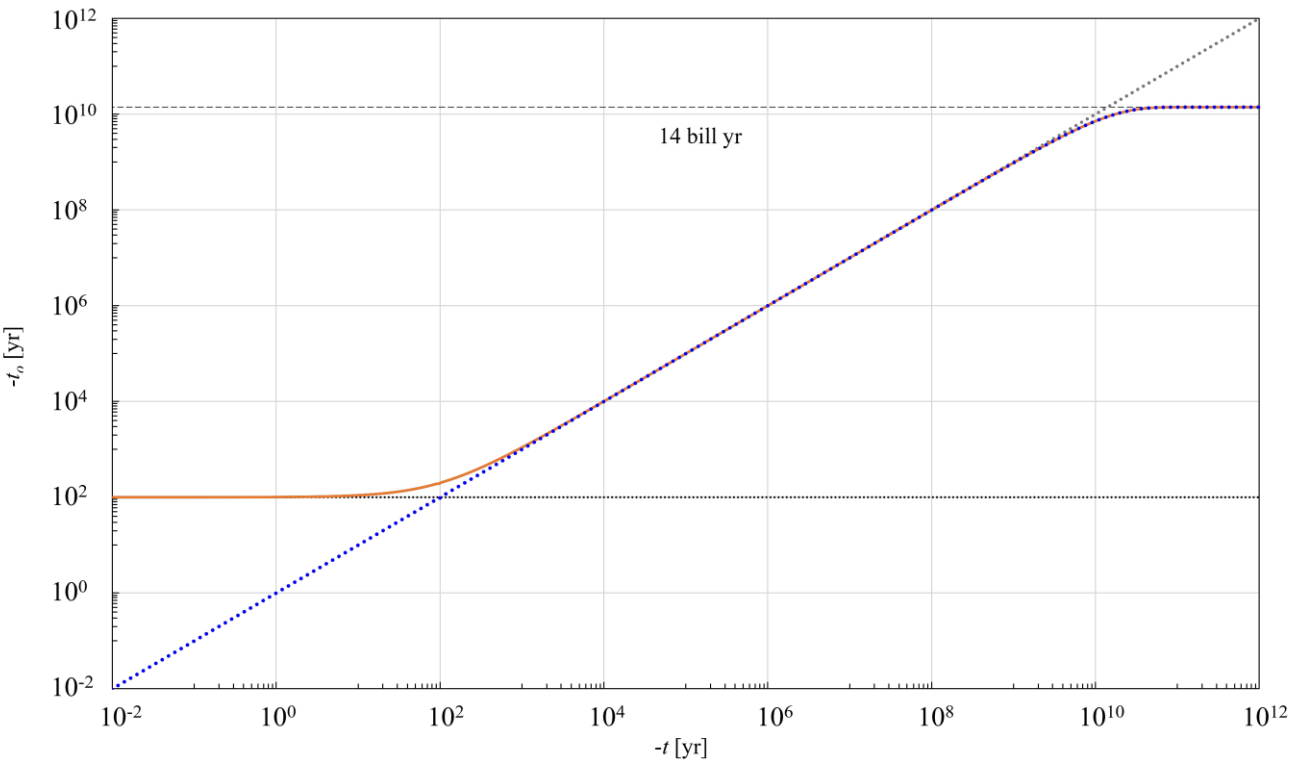

Figure 2. The dependence of the local time t_o on the observation time t of the observer in COP_0 according to (24) (blue dotted curve ·····) shows a significant increase in the dilation of the observation time around 14 billion years (black dashed line -----) into the past, where it forms a kind of boundary that appears in the local time t_o as its beginning. For comparison, the orange curve — shows an observing time against the observer, whose COP_1 is shifted into the past by Δt = 100 yr relative to the first COP (black dotted line ·····).

But what is this limiting value of the apparent "origin" for the observer in COP_1, which is shifted by Δt of observational time into the past relative to the original COP_0 (see Δt = 100 yr in Figure 2)? Due to the conformal metric (21), both minimal time limits t_{00} a t_{10} obey condition

$$\left.\begin{aligned} \mathrm{COP}_0 \to \min t_{00} &= \int_0^{-\infty} e^{Ht} dt = -\frac{1}{H} \\ \mathrm{COP}_1 \to \min t_{10} &= \int_{\Delta t<0}^{-\infty} e^{Ht} dt = -\frac{e^{H\Delta t}}{H} \end{aligned}\right\} \to \boxed{|\min t_{10}| < |\min t_{00}|}. \tag{25}$$

It seems that an observer from COP_1 in the past is closer to this border resembling "age of the universe", than an observer from COP_0. With respect to PREMISE 4, let us denote the equivalent time intervals (transferred local units) by $[\tau_o]$ for COP_o a $[\tau_1]$ for COP_1. In cosmological scales, they can be naturally represented by differentials, so that (23) gives a relationship between the two local units $[\tau_o] \leftrightarrow [\tau_1]$

$$\left.\begin{aligned} dt_o &= e^{Ht} dt \\ dt_1 &= e^{H(t+\Delta t)} dt \end{aligned}\right\} \to dt_1 = e^{H\Delta t} dt_o \to [\tau_1] = e^{H\Delta t} [\tau_o]. \tag{26}$$

While the value of min t_o is naturally expressed in time units $[\tau_o]$ of COP_0, the similarly calculated value of min t_{1o} must be converted into its own time units $[\tau_1]$ COP_1. Let us

compare the dimensionless numbers n_{00} and n_{10} of time units $[\tau_o]$ and $[\tau_1]$ at the "age of the universe" values min t_{00} and min t_{10} from (25)

$$[\tau_1] = e^{H\Delta t}[\tau_0] \rightarrow \left\{ \begin{array}{l} n_{00} = \frac{\min t_{00}}{[\tau_0]} = \left(\frac{1}{H} \cdot \frac{1}{[\tau_0]}\right) \\ n_{10} = \frac{\min t_{10}}{[\tau_1]} = \left(\frac{e^{H\Delta t}}{H} \cdot \frac{1}{e^{H\Delta t}[\tau_0]}\right) = \left(\frac{1}{H} \cdot \frac{1}{[\tau_0]}\right) \end{array} \right\} \rightarrow n_{10} = n_{00} \quad (27)$$

It turns out that for both observers the apparent "age of universe" is the same, so there is no real "beginning of time" in global conformal spacetime. This limit value is the same for all observers (min $t_o \approx -14 \times 10^9$ yr) and the Hubble parameter H is a true universal constant in this model, invariant to time translations.

5. Spatial Distribution of γ-Ray Bursts

Another cosmological test of the conformal Minkowski metric hypothesis can be an experimental verification of the natural homogeneous distribution of matter on a global cosmological scale. Such a test can be performed by observing highly specific astrophysical objects and events such as black holes, quasars, and ultimately γ-ray sources that can be understood as standards (the distribution of galaxies is inappropriate for such a test due to their highly non-standard diversity).

We will discuss the spatial distribution of γ-ray bursts in the following chapter. In [24,25] they published a methodology for applying the $V/V_{\max}$ test to γ-ray sources and subsequently performed a constrained analysis of the spatial distribution for 140 sources [26]. The result shows an increasing deficit in the observed number of low intensity sources. Assuming an identical nature of the sources and the standard Euclidean flat-space metric E3, these results can be interpreted as a decrease in source density towards the past within a fully conformal spacetime. Such an interpretation leads to the conclusion that the γ-ray density changes over time on a global scale.

Let us now perform a similar analysis under a hypothetical conformal metric. The time-independent nature of the energy-momentum tensor (4) requires a global density of γ-ray sources invariant over time. The number of sources N within in a sphere of radius $r_{\max}$ around the COP is given by the time-invariant global source density $n_{\gamma o}$:

$$N(r_{\max}) = n_{\gamma o} \frac{4}{3} \pi r_{\max}^3. \quad (28)$$

In the mentioned $V/V_{\max}$ test [24], the ratio of the intensity $C_{\max} = C(r_{\max})$ of the farthest detected source at distance $r_{\max}$ to the threshold intensity $C_{\min} = \min C$ at the detection limit is chosen as the independently variable distribution parameter. The intensity of the source $C_{\max}$ decreases not only with the inverse square of the distance $r_{\max}$ but also due to the conformal metric (21). As a result, the intensity on a model source surface of radius R decreases with distance $r_{\max}$ from the observer.

Now we analyse the measurement of the "observed intensity" C [J m^{-2} s^{-1}] at distant sources, taking into account the effect of the conformal metric (21). For simplicity, consider a spherical radiation source of radius R. Let us denote by $C_o(R)$ the surface intensity of the radiation in its local inertial system (x_{o1}, x_{o2}, x_{o3}, x_{o4}) (8) and then denote by $C(R)$ the same relative surface intensity of the radiation in the global system (x_1, x_2, x_3, x_4) (8) of the COP at distance r. While the intensity $C(r)$ observed in the COP decreases according to the standard $C(r) \sim 1/r^2$ dependence, the transition between the $C_o(R) \rightarrow C(R)$ intensities is due to the effect of the conformal metric (21) on the intrinsic surface intensity $C_o(R)$. With a suitable orientation of $x_1 = r$, the remaining two space coordinates x_2 and x_3 define a plane perpendicular to the line between source and the COP. The two surface differentials

dS_o and dS of the source surface then lie in this plane, radiating towards the COP, and the relation $C_o(R) \rightarrow C(R)$ can be written as

$$\left.\begin{array}{r} C_0(R) \stackrel{\text{def}}{=} \frac{d^2E}{dS_o dt_o} \\ dS_o = dx_{o2}dx_{o3} \\ C(R) \stackrel{\text{def}}{=} \frac{d^2E}{dSdt} \\ dS = dx_2 dx_3 \end{array}\right\} \rightarrow C(R) = C_0(R)\frac{dS_o dt_o}{dSdt}. \tag{29}$$

As a consequence of the (8), (13) and the conformal metric (21) we can write

$$\left.\begin{array}{r} dx_{o\mu}(x_4) = e^{\frac{H}{c}x_4}dx_\mu \\ x_4 = -r \end{array}\right\} \rightarrow \left\{\begin{array}{r} dx_{o4} = e^{-\frac{H}{c}r}dx_4 \rightarrow dt_o = e^{-\frac{H}{c}r}dt \\ dS_o = dx_{o1}dx_{o2} = e^{-2\frac{H}{c}r}dx_1dx_2 = e^{-2\frac{H}{c}r}dS \end{array}\right\} \rightarrow \frac{dS_o dt_o}{dSdt} = e^{-3\frac{H}{c}r}, \tag{30}$$

and for the relative radiation intensity (29) on a model source surface of radius R it is

$$C(R) = C_o(R)e^{-3\frac{H}{c}r_{\max}}. \tag{31}$$

As a result of the simultaneous decrease in intensity with the square of the distance, Equation (31) takes its final form:

$$\underbrace{C(r_{\max})}_{C_{\max}} \cdot \left(4\pi r_{\max}^2\right) = C(R) \cdot \left(4\pi R^2\right) \rightarrow C_{\max} = C_o(R)\frac{R^2}{r_{\max}^2}e^{-3\frac{H}{c}r_{\max}}. \tag{32}$$

The NSSTC, BATSE4B astrophysical database [27] contains data as dependence of the number of sources on the ratio of the minimum intensity to the threshold intensity $N(C_{\max}/C_{\min})$. To test the conformal metric hypothesis (1), (21), we express Equation (32) in terms of an intensity ratio

$$\frac{C_{\max}}{C_{\min}} = \left(C_o(R)\frac{R^2}{C_{\min}}\right)e^{-3\frac{H}{c}r_{\max}}(r_{\max})^{-2}. \tag{33}$$

The mutual dependence of the two parameters then comes from the simultaneous validity of (28) and (33):

$$\left\{\begin{array}{l} A = \left(\frac{C_o(R)}{C_{\min}}R^2\right)\left(\frac{3}{4\pi n_{\gamma o}}\right)^{-\frac{2}{3}}[-] \\ B = 3\frac{H}{c}\left(\frac{3}{4\pi n_{\gamma o}}\right)^{\frac{1}{3}}[-] \end{array}\right\} \rightarrow \boxed{\frac{C_{\max}}{C_{\min}} = AN^{-\frac{2}{3}}e^{-BN^{\frac{1}{3}}}} \tag{34}$$

The fit of the theoretical dependence (34) to the mentioned experimental data of NSSTC, BATSE4B [27] is shown in Figure 3.

The first requirement of the fit is the limit transition $B \rightarrow 0$ of Formula (34) to the standard version of the Minkowski metric for small distances from the COP, which shows asymptotic behaviour for well-detectable sources with large $C_{\max}$ corresponding to smaller $r_{\max}$. The coefficient of determination $R^2 \approx 0.888$ demonstrates approximately 90% fit of the regression model function to the observational data in the region $C_{\max}/C_{\min} \geq 10$. The above fit for $B = 0.12$ gives a time-invariant global γ-ray burst density of $n_{\gamma o} \approx 1.47 \times 10^{-75}$ m^{-3} ≈ 43 Gpc^{-3} according to (34).

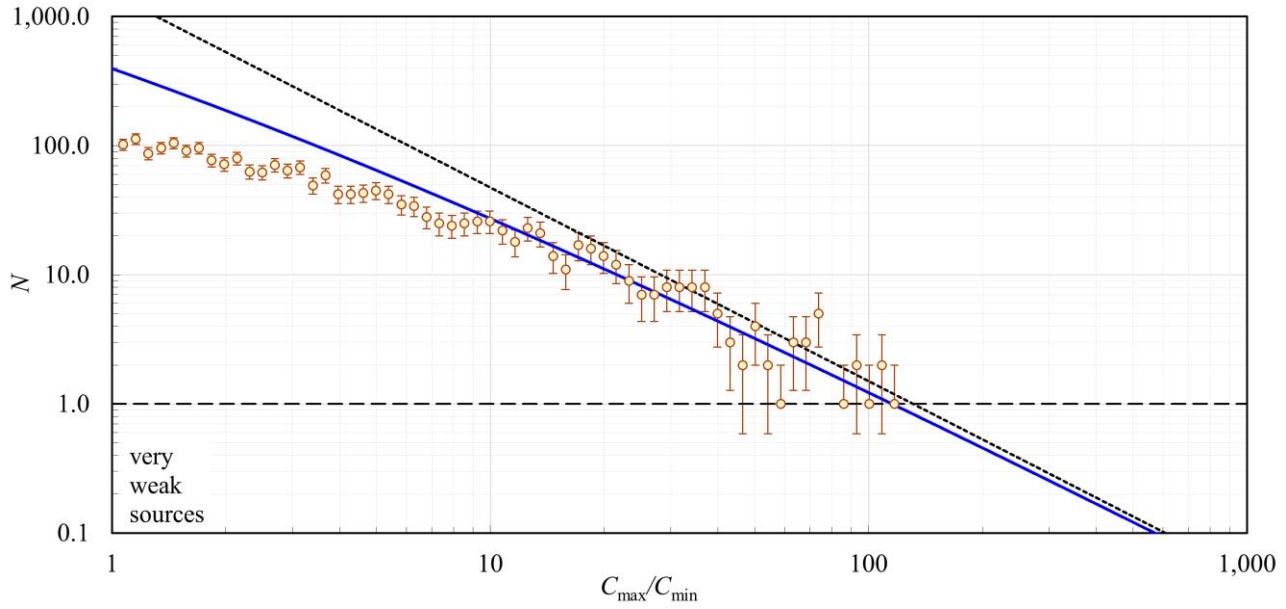

Figure 3. Theoretical fit — distribution of the total number N of γ-ray burst sources as a function of the C_{max}/C_{min} ratio for 2372 measured sources (A = 130, B = 0.12)—orange points. The black dashed line would correspond to a uniform distribution of sources in flat space with the standard Euclidean metric E3, as indicated by a formal extrapolation of the plot below the single-source detection level of N = 1.

The detection of the vast majority of strong sources in the nearby region ($C_{max}/C_{min} \geq 10$) is highly probable both in terms of their high intensity and their frequency of occurrence in a relatively small volume of the vicinity of the COP. However, in more distant regions, the detection probability is negatively affected both by the decreasing intensity of the sources and by their more difficult localization in an extremely increasing volume. In the Gaussian angular distribution of the intensity of narrow γ-ray bursts [28], the minimum measurable intensity C_{min} determines the edge of the Gaussian profile, so the effective solid angle detection of the γ-ray burst decreases with distance. This naturally reduces the probability of passage through the ground-based observation point and hence the frequency of detected sources. Detection of "missing" sources could therefore serve as one way to verify or falsify this hypothesis of a global conformal metric of the universe.

6. Spatial Distribution of Quasars

D. Sciama and M. Rees published a paper in 1966 [29] with the intention of falsifying the steady state theory of the universe. The paper showed that the frequency of observed quasars depends on the magnitude of the redshift, and from this fact, they deduced a time evolution of the source density that contradicts the ideas of the steady-state model of the universe. This raises the question of how to correctly interpret observations of sources with different redshift values. Although the estimated time evolution of the source density was contrary to steady-state concepts, it has not been explained in principle even within the standard ΛCMD cosmological model. It is associated with the general assumption of the genesis and evolution of astrophysical objects within any cosmological theory with a time origin. Of course, the time evolution cannot be excluded even in models without said beginning, because with limited observational experience, we may miss slow global processes ("Too brief glimpse into the past from the beginning of summer may lead one to believe that the world was created in winter").

Thus, we examine whether the hypothesis of the conformal metric is consistent with the assumption that the distribution of quasars seems to be homogeneous in space from the

COP. For a time-invariant global source density n_{qo}, the number of sources dN contained in a differential spherical shell of radius r around the COP is given by

$$dN = n_{qo} 4\pi r^2 dr. \tag{35}$$

Now we derive the distribution of dN/dz as a function of redshift from all observed quasars. From the generalized Hubble–Lemaître law (20), the radial parameters r and dr on the right-hand side of Equation (35) can be expressed as a function of the redshift z

$$z = e^{\frac{H}{c}r} - 1 \rightarrow \begin{cases} r = \frac{c}{H}\ln(z+1) \\ \frac{dz}{dr} = \frac{H}{c}e^{\frac{H}{c}r} \rightarrow dr = \frac{c}{H}e^{-\frac{H}{c}r}dz \rightarrow dr = \frac{c}{H}\frac{dz}{z+1} \end{cases}. \tag{36}$$

Substitution into (35) then gives the final formula for comparison with experimental data

$$A = 4\pi n_{qo}\left(\frac{c}{H}\right)^3 \rightarrow \boxed{\frac{dN}{dz} = A\frac{(\ln(z+1))^2}{z+1}}. \tag{37}$$

The relevant data were used from The Million Quasars (Milliquas) catalog, v7.2aa, 18 October 2021 [30], which contains experimental data obtained by observing about 977,000 sources. The fit of the theoretical dependence (37) to these experimental data is shown in Figure 4.

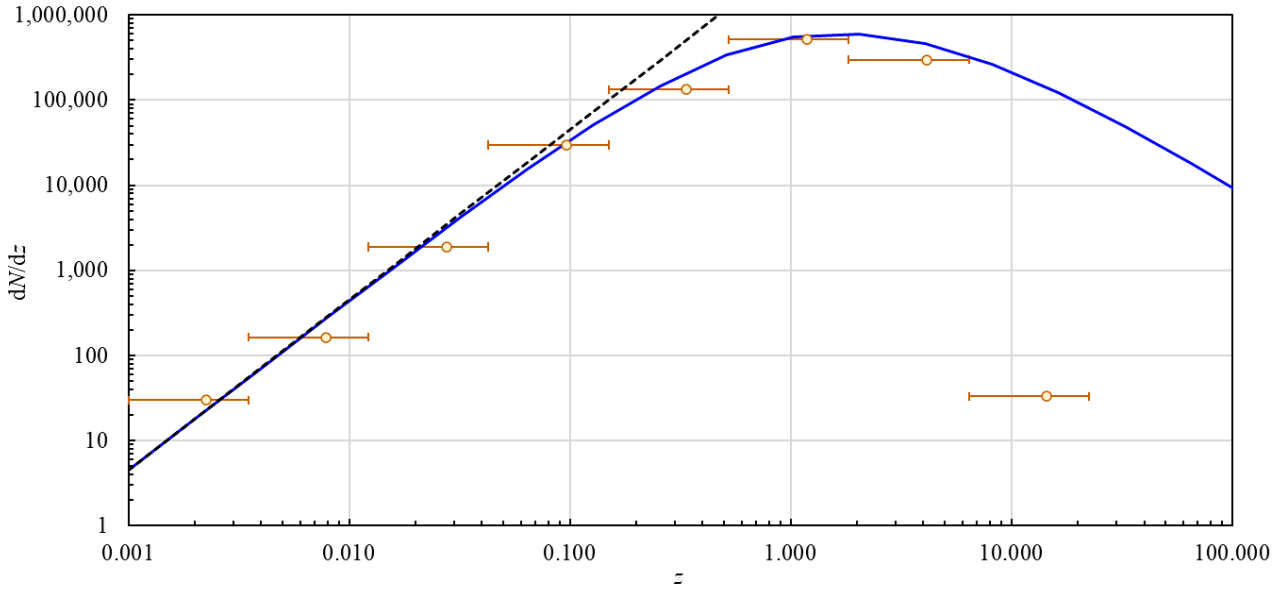

Figure 4. Theoretical fit — of the dependence of the number of quasars with the increase in redshift dN/dz on the magnitude of their redshift z (for parameter 4.5×10^6) [30]. Hollow orange points correspond to the average of all measured z values within the respective interval, and the horizontal line defines its width. The black dashed line **---** corresponds to a uniform distribution of sources in flat space with Euclidean metric E3 and the standard linear form of Hubble–Lemaître law for redshift.

The requirement of the fit is again the limit transition $z \rightarrow 0$ of Equation (37) to the standard version of the Minkowski metric at small distances from the COP. This requirement of asymptotic behaviour is satisfied by the transition of the function (37) to the standard form z^2. The theoretical shape of the fit function is confronted in good agreement with the number of nearer quasars in the first six statistical intervals, which are shown in Figure 4 as horizontal lines.

The calculated coefficient of determination $R^2 \approx 0.9511$ demonstrates approximately 95% fit of the regression model function to the observational data for the first six points.

Using the regression parameter $A \approx 4.5 \times 10^6$ in Equation (37) we can estimate the quasar number density in the universe to $n_{q0} \approx 1.55 \times 10^{-73}$ m$^{-3} \approx 4559$ Gpc^{-3}.

Similarly to the previous section, we can also justify the deficit in the number of sources in the last interval for high values of z. And again, additional measurements could serve to partially verify, or refute the hypothesis of a global conformal metric of the universe.

All the model predictions with observational data in Sections 3, 5 and 6 documents approximately a 90% fit or better. To consider such a degree of coincidence as the work of chance seems very problematic. What conclusions can be drawn from this? The analysis of the "selected data sets" seems to confirm with a high probability the validity of the "perfect cosmological principle", which was the initial assumption for the theoretical derivation of the respective formulae (20), (34) and (37). At the same time, all three formulae provide predictions for high redshift z values above the "selected data sets". These outlying regions are currently characterised by a deficit of observed objects, so model predictions can be used to subsequently verify the homogeneous space-time distribution that was the basic and simplest assumption of the steady state. This hypothesis of a homogeneous spatio-temporal distribution of astrophysical objects can be considered much more robust than current ideas of evolution, which are often problematised by recent observational data from the James Webb Space Telescope and others.

7. Olbers' Paradox and the Observable Universe

The assumption of a luminous sky in the visible light region does not match experimental experience (Olbers' paradox), and in a universe with a fully conformal metric (1) this paradox can be explained via redshift. Assume that on sufficiently large cosmological scales the number density of model astrophysical light sources n can be approximated by a constant. We introduce the intensity contribution dI_Ω of the average model sources from the differential volume $dV = d\Omega r^2 dr$ at distance r from the COP, oriented towards the COP, which is given by the emission of radiative energy ε from the source surface to the differential solid angle $d\Omega$

$$dI_\Omega(r) = \left(\frac{d^2\varepsilon(r)}{dt(r)dS(r)}\right) n d\Omega r^2 dr. \tag{38}$$

As a result of the metric transformation of the derivative variables (30), it decreases exponentially with distance r from the COP

$$\left\{\frac{dt(0)dS(0)}{dt(r)dS(r)} = e^{-3\frac{H}{c}r}\right\} \rightarrow dI_\Omega(r) = \left(\frac{d^2\varepsilon(r)}{dt(0)dS(0)}\right) e^{-3\frac{H}{c}r} n d\Omega r^2 dr. \tag{39}$$

For simplicity of the model derivation, assume purely thermal emission from an average model source with surface temperature $T(0)$. After including all the mentioned effects, the intensity contribution dI_Ω (39) takes the form

$$\left.\begin{array}{l}\text{inverse square law} \rightarrow \frac{d^2\varepsilon(r)}{dt(0)dS(0)} = \left(\frac{\sigma}{\pi}T(r)^4\right)\frac{1}{r^2} \\ \text{redshift} + \text{Wien's law} \rightarrow \frac{T(r)}{T(0)} = \frac{\nu_{\max}(r)}{\nu_{\max}(0)} = e^{-\frac{H}{c}r}\end{array}\right\} \rightarrow dI_\Omega(r) = \left(\frac{\sigma}{\pi}T(0)^4\right) e^{-7\frac{H}{c}r} n d\Omega dr. \tag{40}$$

The experimentally measured intensity $I_\Omega(R)$ [Wm^{-2}sr^{-1}] in the direction of the unit angle axis is the sum of all contributions from the opposite half-space 2π to the distance R of the observation horizon

$$I_\Omega(R) = \iiint\limits_{V_R^{2\pi}} dI_\Omega = \int_0^{2\pi}\int_0^R \left(\frac{\sigma}{\pi}T(0)^4\right) e^{-7\frac{H}{c}r} n d\Omega dr = 2\pi\left(\frac{\sigma}{\pi}T(0)^4\right) n \left(\int_0^R e^{-7\frac{H}{c}r} dr\right) \tag{41}$$

Without knowledge of the model parameters n and $T(0)$, the dependence of the intensity $I_\Omega(R)$ on the distance R from the COP can be characterized by the function $\Phi(R)$, which is defined by the parametric integral in (41)

$$\Phi(R) = \int_0^R e^{-7\frac{H}{c}r}\, dr = \frac{c}{7H}\left(1 - e^{-7\frac{H}{c}R}\right), \tag{42}$$

and its graph is shown in Figure 5.

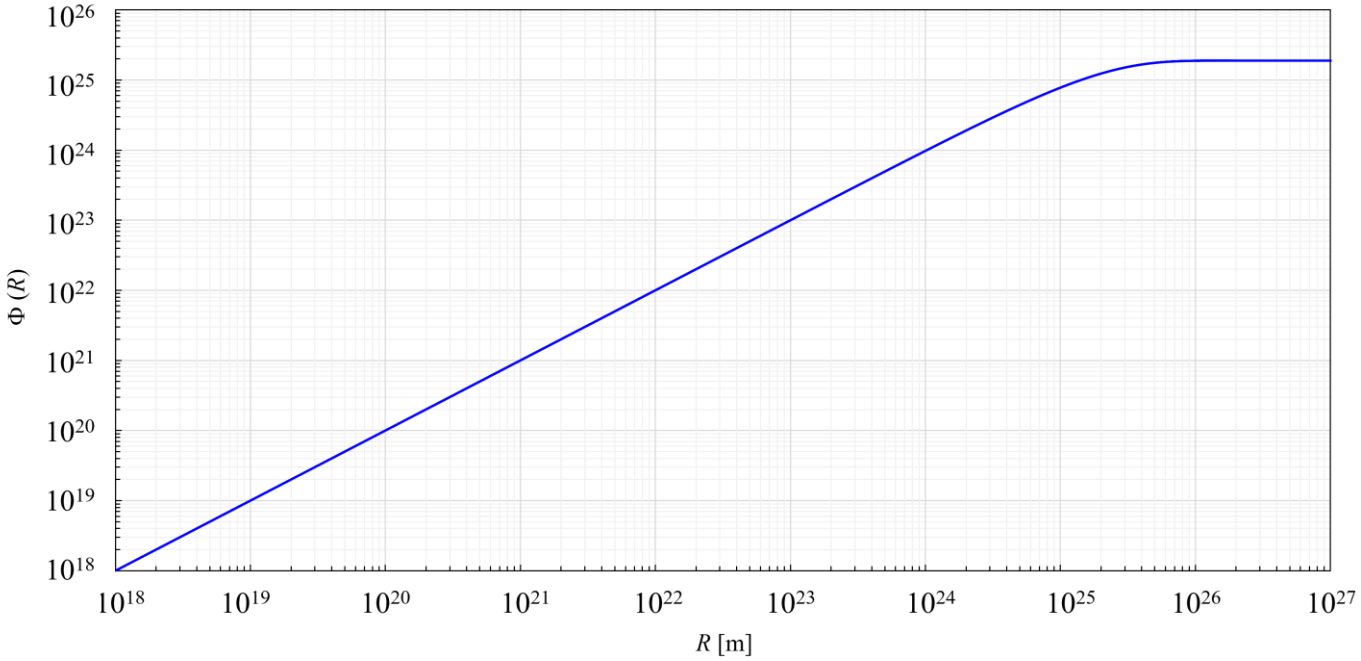

Figure 5. Dependence of the function $\Phi(R)$ (42) on the distance R of the observation sphere from the COP. The asymptotic plateau of the total intensity corresponds to a slightly smaller radius than predicted $R_{obs} \approx 4.3 \times 10^{26}$ m by the calculations of the standard model [31].

The asymptotic behaviour of the dependence (42) leads to the final value of the total intensity max I_Ω

$$\max I_\Omega(R) = \lim_{R\to\infty} I_\Omega(R) = 2n\sigma T(0)^4 \cdot \lim_{R\to\infty} \Phi(R) \to \boxed{\max I_\Omega(R) = 2n\sigma T(0)^4 \frac{c}{7H} \ll \infty}, \tag{43}$$

which is approximately reached already at distances of the order of $R \approx 10^{26}$ m, and the outer region contributes negligibly. This is how the problem of the Olbers' paradox is solved within the fully conformal metric.

While in a space with a standard Minkowski metric the radiation of all differential spheres would contribute equally to the total intensity at the COP, under the conditions of a conformal metric there is a kind of limit at which the differential contributions to the total intensity drop significantly to negligible values. This decrease can be expressed on the basis of relation (40) in the form of function

$$\Psi(r) = \frac{dI_\Omega(r)/dr}{dI_\Omega(0)/dr} = e^{-7\frac{H}{c}r} \tag{44}$$

The dependence (44) is plotted in Figure 6. The radial distance $r = 4 \times 10^{26}$ m from the COP; at which the intensity contribution drops by nine orders of magnitude to 1 ppb of the

original value; agrees very well with the $R_{obs} \approx 4.3 \times 10^{26}$ m of the observable universe according to the standard model [31].

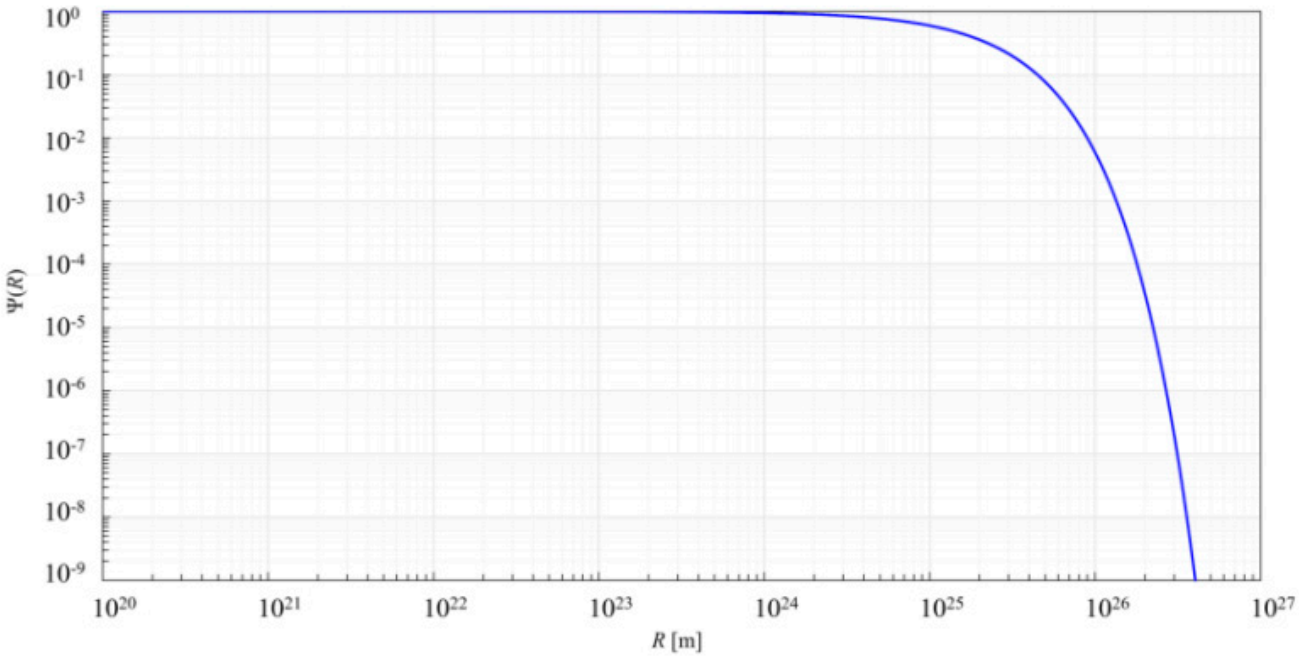

Figure 6. Dependence of the relative intensity decrease function $\Psi(R)$ (44) on the distance R from the COP.

The fully conformal metric thus defines a region of the observable universe where the contributions from the outer region are not zero in principle as in the case of causal cosmological horizon of the standard model, but they are completely negligible from an energy perspective. According to one of the most recent observations from the James Webb Telescope in 2022 [32], we can consider detecting objects with redshifts up to $z = 12$, which according to (20), corresponds to a distance of 3.5×10^{26} m located the steep intensity drop of eight orders of magnitude in Figure 6.

8. Conclusions

This paper presents a scale invariant fully conformal cosmological model based on a new physical interpretation of the relatively simple global solution of Einstein's gravitational equations with a time-independent energy-momentum tensor. This solution takes the form of a fully conformal Minkowski metric that is globally scaled by the same time function $\psi(x_4)$ in all four space-time coordinates. The time dependences of the metric tensor $g_{\mu\nu}(x_4)$ in the components of the Einstein tensor on the left-hand side of the gravity equations are fully compensated in accordance with the time-independent components of the energy-momentum tensor on the right-hand side. The above conformal metric preserves the time independence of the speed of light, and similar to the rest mass, other local physical parameters such as the electromagnetic spectrum etc. are conserved around an arbitrary COP. Clocks and gauges in the vicinity of all COPs must also be viewed as fully equivalent, and the universe on a global scale as stationary spacetime is scale invariant, and exponential expansion is only relative observational in nature. The changes in scales and time flow observed over large distances (in the past) are only relative to a given COP, like the relativistic change in mass of particles in motion. Given the universal nature of the local quantum definition of the time unit 1s and the possibility of naturally choosing the origin of the COP ($x_4 = 0$) in the local presence of an arbitrary observer, the exponential form of the scaling function $\psi(x_4)$ is covariant. Instead of a real time origin, the model

introduces the "appearent age of the universe", which, due to dilation, is the limiting value of the time parameter towards the past and corresponds to the present value of the "age of the universe" H^{-1} according to the standard model. This "appearent age" is the same for all observers at different time levels, and the Hubble parameter is thus a true universal constant, invariant to time translations. The experimental part of the paper then discusses some observational implications of the presented model. Without the need for a cosmological term in Einstein's gravity equations, the model provides a physical interpretation for the formulation of the generalized Hubble-Lemaître law $z(r) = (e^{Hr/c} - 1)$, which agrees very well with current astrophysical data even for very distant supernovae Ia. The whole concept was motivated by considerations of whether cosmological redshifts can arise in the time evolution of the global metric field due to its differences at different time levels, similar to the case of gravitational redshifts in the radiation emission of very massive objects. The question of an alternative interpretation of the cosmological redshift has been raised in the past by Fritz Zwicky. However, his concept of "tired light" corresponded to a gravitational redshift based on the local curvature of spacetime by the masses of galaxies, and the redshift depended on the local spatial distances from the galactic centers. This does not agree with the observations that showed a global dependence of the redshift on the distance from any observer, regardless of the distribution of masses. On the other hand, the global conformal solution shows interesting agreement with experimental observations of the spatial distribution of real astrophysical sources such as γ-ray bursts and quasars. The conformal metric field model also solves in principle the problem of critical global density, flatness of 3D space and Olbers' paradox. The strictly sharp cosmological horizon in the standard model is here replaced by a much softer formulation a region of the practically observable universe, that is not bounded by a sharp causal boundary. The follow-up work will focus on the generalization of the Schwartschild solution based on the background of the above fully conformal metric, the derivation of the corresponding equation of state, and a description of the origin of the CMB.

Funding: For Region Sustainability and High-tech Industries project number CZ.10.03.01/00/22_003/0000048 via the Operational Programme Just Transition. I thank, to my colleague Jiri Bednar for his careful review and preparation of the English text, and first and foremost I am very grateful to Jeyninka for great support in my work.

Data Availability Statement: NASA (1996) Gamma-Ray Astrophysics: NSSTC, BATSE4B, CMAXMIN TABLE. Available at: https://gammaray.nsstc.nasa.gov/batse/grb/catalog/4b/4br_cmax_cmin.html. NASA (2022) NASA/IPAC EXTRAGALACTIC DATABASE (2022): Date and Time of the Query: Sun Nov 12 09:25:30 2017PDT. Available at: https://ned.ipac.caltech.edu/. Planck 2013 (2013) Planck 2013 results.: I. Overview of products and scientific results, Astronomy & Astrophysics manuscript no. Planck Mission. Available at: https://arxiv.org/pdf/1303.5062.pdf.

Acknowledgments: The work was supported by the project No. CZ.02.01.01/00/22_008/0004631. Materials and technologies for sustainable development within the Jan Amos Komensky Operational Program financed by the European Union and from the state budget of the Czech Republic and the European Union under the REFRESH—Research Excellence For Region Sustainability and High-tech Industries project number CZ.10.03.01/00/22_003/0000048 via the Operational Programme Just Transition. I thank, to my colleague Jiri Bednar for his careful review and preparation of the English text, and first and foremost I am very grateful to Jeyninka for great support in my work.

Conflicts of Interest: The author declares no conflict of interest.

Appendix A

M4 - space

$$\Gamma^{\mu}{}_{\nu\lambda} = \frac{1}{2} g^{\mu\alpha} \left(\partial_{\nu} g_{\alpha\lambda} + \partial_{\lambda} g_{\alpha\nu} - \partial_{\alpha} g_{\nu\lambda} \right)$$

$$\boxed{\Gamma^{\mu}{}_{\nu\lambda} = \frac{1}{2} g^{\mu 1} \left(\partial_{\nu} g_{1\lambda} + \partial_{\lambda} g_{1\nu} \right) + \frac{1}{2} g^{\mu 2} \left(\partial_{\nu} g_{2\lambda} + \partial_{\lambda} g_{2\nu} \right) + \frac{1}{2} g^{\mu 3} \left(\partial_{\nu} g_{3\lambda} + \partial_{\lambda} g_{3\nu} \right) + \frac{1}{2} g^{\mu 4} \left(\partial_{\nu} g_{4\lambda} + \partial_{\lambda} g_{4\nu} - \partial_{4} g_{\nu\lambda} \right)}$$

$$\boxed{\begin{array}{l} g_{11}(x_4) = \psi(x_4)\eta_{11} = \psi(x_4) \\ g_{22}(x_4) = \psi(x_4)\eta_{22} = \psi(x_4) \\ g_{33}(x_4) = \psi(x_4)\eta_{33} = \psi(x_4) \\ g_{44}(x_4) = \psi(x_4)\eta_{44} = -\psi(x_4) \end{array}}$$

$$\Gamma^{1}{}_{\nu\lambda} = \frac{1}{2} g^{11} \left(\partial_{\nu} g_{1\lambda} + \partial_{\lambda} g_{1\nu} \right) \rightarrow \begin{cases} \Gamma^{1}{}_{1\lambda} = \frac{1}{2} g^{11} \left(\underbrace{\partial_{1} g_{1\lambda}}_{0} + \partial_{\lambda} g_{11} \right) = \frac{1}{2} g^{11} \partial_{\lambda} g_{11} \rightarrow \boxed{\Gamma^{1}{}_{14} = \frac{1}{2} g^{11} \partial_{4} g_{11} \rightarrow \Gamma^{1}{}_{14} = \frac{1}{2} \psi(x_4)^{-1} \partial_{4} \psi(x_4)} \\ \Gamma^{1}{}_{2\lambda} = \frac{1}{2} g^{11} \left(\underbrace{\partial_{2} g_{1\lambda}}_{0} + \partial_{\lambda} \underbrace{g_{12}}_{0} \right) = 0 \\ \Gamma^{1}{}_{3\lambda} = \frac{1}{2} g^{11} \left(\underbrace{\partial_{3} g_{1\lambda}}_{0} + \partial_{\lambda} \underbrace{g_{13}}_{0} \right) = 0 \\ \Gamma^{1}{}_{4\lambda} = \frac{1}{2} g^{11} \left(\partial_{4} g_{1\lambda} + \partial_{\lambda} \underbrace{g_{14}}_{0} \right) = \frac{1}{2} g^{11} \partial_{4} g_{1\lambda} \rightarrow \boxed{\Gamma^{1}{}_{41} = \frac{1}{2} g^{11} \partial_{4} g_{11} \rightarrow \Gamma^{1}{}_{41} = \frac{1}{2} \psi(x_4)^{-1} \partial_{4} \psi(x_4)} \end{cases}$$

$$\Gamma^{2}{}_{\nu\lambda} = \frac{1}{2} g^{22} \left(\partial_{\nu} g_{2\lambda} + \partial_{\lambda} g_{2\nu} \right) \rightarrow \begin{cases} \Gamma^{2}{}_{1\lambda} = \frac{1}{2} g^{22} \left(\underbrace{\partial_{1} g_{2\lambda}}_{0} + \partial_{\lambda} \underbrace{g_{21}}_{0} \right) = 0 \\ \Gamma^{2}{}_{2\lambda} = \frac{1}{2} g^{22} \left(\underbrace{\partial_{2} g_{2\lambda}}_{0} + \partial_{\lambda} g_{22} \right) = \frac{1}{2} g^{22} \partial_{\lambda} g_{22} \rightarrow \boxed{\Gamma^{2}{}_{24} = \frac{1}{2} g^{22} \partial_{4} g_{22} \rightarrow \Gamma^{2}{}_{24} = \frac{1}{2} \psi(x_4)^{-1} \partial_{4} \psi(x_4)} \\ \Gamma^{2}{}_{3\lambda} = \frac{1}{2} g^{22} \left(\underbrace{\partial_{3} g_{2\lambda}}_{0} + \partial_{\lambda} \underbrace{g_{23}}_{0} \right) = 0 \\ \Gamma^{2}{}_{4\lambda} = \frac{1}{2} g^{22} \left(\partial_{4} g_{2\lambda} + \partial_{\lambda} \underbrace{g_{24}}_{0} \right) = \frac{1}{2} g^{22} \partial_{4} g_{2\lambda} \rightarrow \boxed{\Gamma^{2}{}_{42} = \frac{1}{2} g^{22} \partial_{4} g_{22} \rightarrow \Gamma^{2}{}_{42} = \frac{1}{2} \psi(x_4)^{-1} \partial_{4} \psi(x_4)} \end{cases}$$

$$\Gamma^{3}{}_{\nu\lambda} = \frac{1}{2} g^{33} \left(\partial_{\nu} g_{3\lambda} + \partial_{\lambda} g_{3\nu} \right) \rightarrow \begin{cases} \Gamma^{3}{}_{1\lambda} = \frac{1}{2} g^{33} \left(\underbrace{\partial_{1} g_{3\lambda}}_{0} + \partial_{\lambda} \underbrace{g_{31}}_{0} \right) = 0 \\ \Gamma^{3}{}_{2\lambda} = \frac{1}{2} g^{33} \left(\underbrace{\partial_{2} g_{3\lambda}}_{0} + \partial_{\lambda} \underbrace{g_{32}}_{0} \right) = 0 \\ \Gamma^{3}{}_{3\lambda} = \frac{1}{2} g^{33} \left(\underbrace{\partial_{3} g_{3\lambda}}_{0} + \partial_{\lambda} g_{33} \right) = \frac{1}{2} g^{33} \partial_{\lambda} g_{33} \rightarrow \boxed{\Gamma^{3}{}_{34} = \frac{1}{2} g^{33} \partial_{4} g_{33} \rightarrow \Gamma^{3}{}_{34} = \frac{1}{2} \psi(x_4)^{-1} \partial_{4} \psi(x_4)} \\ \Gamma^{3}{}_{4\lambda} = \frac{1}{2} g^{33} \left(\partial_{4} g_{3\lambda} + \partial_{\lambda} \underbrace{g_{34}}_{0} \right) = \frac{1}{2} g^{33} \partial_{4} g_{3\lambda} \rightarrow \boxed{\Gamma^{3}{}_{43} = \frac{1}{2} g^{33} \partial_{4} g_{33} \rightarrow \Gamma^{3}{}_{43} = \frac{1}{2} \psi(x_4)^{-1} \partial_{4} \psi(x_4)} \end{cases}$$

$$\Gamma^{4}{}_{\nu\lambda} = \frac{1}{2} g^{44} \left(\partial_{\nu} g_{4\lambda} + \partial_{\lambda} g_{4\nu} - \partial_{4} g_{\nu\lambda} \right) \rightarrow \begin{cases} \Gamma^{4}{}_{1\lambda} = \frac{1}{2} g^{44} \left(\underbrace{\partial_{1} g_{4\lambda}}_{0} + \partial_{\lambda} \underbrace{g_{41}}_{0} - \partial_{4} g_{1\lambda} \right) = -\frac{1}{2} g^{44} \partial_{4} g_{1\lambda} \rightarrow \boxed{\begin{array}{l} \Gamma^{4}{}_{11} = -\frac{1}{2} g^{44} \partial_{4} g_{11} \rightarrow \\ \Gamma^{4}{}_{11} = \frac{1}{2} \psi(x_4)^{-1} \partial_{4} \psi(x_4) \end{array}} \\ \Gamma^{4}{}_{2\lambda} = \frac{1}{2} g^{44} \left(\underbrace{\partial_{2} g_{4\lambda}}_{0} + \partial_{\lambda} \underbrace{g_{42}}_{0} - \partial_{4} g_{2\lambda} \right) = -\frac{1}{2} g^{44} \partial_{4} g_{2\lambda} \rightarrow \boxed{\begin{array}{l} \Gamma^{4}{}_{22} = -\frac{1}{2} g^{44} \partial_{4} g_{22} \rightarrow \\ \Gamma^{4}{}_{22} = \frac{1}{2} \psi(x_4)^{-1} \partial_{4} \psi(x_4) \end{array}} \\ \Gamma^{4}{}_{3\lambda} = \frac{1}{2} g^{44} \left(\underbrace{\partial_{3} g_{4\lambda}}_{0} + \partial_{\lambda} \underbrace{g_{43}}_{0} - \partial_{4} g_{3\lambda} \right) = -\frac{1}{2} g^{44} \partial_{4} g_{3\lambda} \rightarrow \boxed{\begin{array}{l} \Gamma^{4}{}_{33} = -\frac{1}{2} g^{44} \partial_{4} g_{33} \rightarrow \\ \Gamma^{4}{}_{33} = \frac{1}{2} \psi(x_4)^{-1} \partial_{4} \psi(x_4) \end{array}} \\ \Gamma^{4}{}_{4\lambda} = \frac{1}{2} g^{44} \left(\partial_{4} g_{4\lambda} + \partial_{\lambda} g_{44} - \partial_{4} g_{4\lambda} \right) \rightarrow \boxed{\Gamma^{4}{}_{44} = \frac{1}{2} g^{44} \partial_{4} g_{44} \rightarrow \Gamma^{4}{}_{44} = \frac{1}{2} \psi(x_4)^{-1} \partial_{4} \psi(x_4)} \end{cases}$$

Appendix B

E3 - space

$$\Gamma^{\mu}{}_{\nu\lambda} = \frac{1}{2} g^{\mu\alpha} \left(\partial_{\nu} g_{\alpha\lambda} + \partial_{\lambda} g_{\alpha\nu} - \partial_{\alpha} g_{\nu\lambda} \right)$$

$$\boxed{\Gamma^{\mu}{}_{\nu\lambda} = \frac{1}{2} g^{\mu 1} \left(\partial_{\nu} g_{1\lambda} + \partial_{\lambda} g_{1\nu} \right) + \frac{1}{2} g^{\mu 2} \left(\partial_{\nu} g_{2\lambda} + \partial_{\lambda} g_{2\nu} \right) + \frac{1}{2} g^{\mu 3} \left(\partial_{\nu} g_{3\lambda} + \partial_{\lambda} g_{3\nu} \right)}$$

$$\Gamma^{1}{}_{\nu\lambda} = \frac{1}{2} g^{11} \left(\partial_{\nu} g_{1\lambda} + \partial_{\lambda} g_{1\nu} \right) \rightarrow \begin{cases} \Gamma^{1}{}_{1\lambda} = \frac{1}{2} g^{11} \left(\underbrace{\partial_{1} g_{1\lambda}}_{0} + \partial_{\lambda} g_{11} \right) = \frac{1}{2} g^{11} \partial_{\lambda} g_{11} = 0 \\ \Gamma^{1}{}_{2\lambda} = \frac{1}{2} g^{11} \left(\underbrace{\partial_{2} g_{1\lambda}}_{0} + \partial_{\lambda} \underbrace{g_{12}}_{0} \right) = 0 \\ \Gamma^{1}{}_{3\lambda} = \frac{1}{2} g^{11} \left(\underbrace{\partial_{3} g_{1\lambda}}_{0} + \partial_{\lambda} \underbrace{g_{13}}_{0} \right) = 0 \end{cases}$$

$$\Gamma^{2}{}_{\nu\lambda} = \frac{1}{2} g^{22} \left(\partial_{\nu} g_{2\lambda} + \partial_{\lambda} g_{2\nu} \right) \rightarrow \begin{cases} \Gamma^{2}{}_{1\lambda} = \frac{1}{2} g^{22} \left(\underbrace{\partial_{1} g_{2\lambda}}_{0} + \partial_{\lambda} \underbrace{g_{21}}_{0} \right) = 0 \\ \Gamma^{2}{}_{2\lambda} = \frac{1}{2} g^{22} \left(\underbrace{\partial_{2} g_{2\lambda}}_{0} + \partial_{\lambda} g_{22} \right) = \frac{1}{2} g^{22} \partial_{\lambda} g_{22} = 0 \\ \Gamma^{2}{}_{3\lambda} = \frac{1}{2} g^{22} \left(\underbrace{\partial_{3} g_{2\lambda}}_{0} + \partial_{\lambda} \underbrace{g_{23}}_{0} \right) = 0 \end{cases}$$

$$\Gamma^{3}{}_{\nu\lambda} = \frac{1}{2} g^{33} \left(\partial_{\nu} g_{3\lambda} + \partial_{\lambda} g_{3\nu} \right) \rightarrow \begin{cases} \Gamma^{3}{}_{1\lambda} = \frac{1}{2} g^{33} \left(\underbrace{\partial_{1} g_{3\lambda}}_{0} + \partial_{\lambda} \underbrace{g_{31}}_{0} \right) = 0 \\ \Gamma^{3}{}_{2\lambda} = \frac{1}{2} g^{33} \left(\underbrace{\partial_{2} g_{3\lambda}}_{0} + \partial_{\lambda} \underbrace{g_{32}}_{0} \right) = 0 \\ \Gamma^{3}{}_{3\lambda} = \frac{1}{2} g^{33} \left(\underbrace{\partial_{3} g_{3\lambda}}_{0} + \partial_{\lambda} g_{33} \right) = \frac{1}{2} g^{33} \partial_{\lambda} g_{33} = 0 \end{cases}$$

Appendix C

M4 - space

$$R_{\lambda\nu} = \partial_{\mu}\Gamma^{\mu}{}_{\nu\lambda} - \partial_{\nu}\Gamma^{\mu}{}_{\mu\lambda} + \Gamma^{\eta}{}_{\nu\lambda}\Gamma^{\mu}{}_{\mu\eta} - \Gamma^{\eta}{}_{\mu\lambda}\Gamma^{\mu}{}_{\nu\eta} \rightarrow \begin{cases} R_{11} = \partial_4\Gamma^4{}_{11} + \Gamma^{\eta}{}_{11}\Gamma^{\mu}{}_{\mu\eta} - \Gamma^{\eta}{}_{\mu 1}\Gamma^{\mu}{}_{1\eta} \\ R_{22} = \partial_4\Gamma^4{}_{22} + \Gamma^{\eta}{}_{22}\Gamma^{\mu}{}_{\mu\eta} - \Gamma^{\eta}{}_{\mu 2}\Gamma^{\mu}{}_{2\eta} \\ R_{33} = \partial_4\Gamma^4{}_{33} + \Gamma^{\eta}{}_{33}\Gamma^{\mu}{}_{\mu\eta} - \Gamma^{\eta}{}_{\mu 3}\Gamma^{\mu}{}_{3\eta} \\ R_{44} = \partial_4\Gamma^4{}_{44} - \partial_4\Gamma^{\mu}{}_{\mu 4} + \Gamma^{\eta}{}_{44}\Gamma^{\mu}{}_{\mu\eta} - \Gamma^{\eta}{}_{\mu 4}\Gamma^{\mu}{}_{4\eta} \end{cases}$$

$$\boxed{R_{11} = \boxed{\partial_1\Gamma^1{}_{11} + \partial_2\Gamma^2{}_{11} + \partial_3\Gamma^3{}_{11}} + \partial_4\Gamma^4{}_{11} + \Gamma^{\eta}{}_{11}\Gamma^{\mu}{}_{\mu\eta} - \Gamma^{\eta}{}_{\mu 1}\Gamma^{\mu}{}_{1\eta}}$$

$$R_{11} = \partial_4\Gamma^4{}_{11} + \begin{bmatrix} \left(\Gamma^1{}_{11}\Gamma^1{}_{11} - \Gamma^1{}_{11}\Gamma^1{}_{11}\right) + \left(\Gamma^1{}_{11}\Gamma^2{}_{21} - \Gamma^1{}_{21}\Gamma^2{}_{11}\right) + \left(\Gamma^1{}_{11}\Gamma^3{}_{31} - \Gamma^1{}_{31}\Gamma^3{}_{11}\right) + \left(\Gamma^1{}_{11}\Gamma^4{}_{41} - \Gamma^1{}_{41}\Gamma^4{}_{11}\right) \\ + \left(\Gamma^2{}_{11}\Gamma^1{}_{12} - \Gamma^2{}_{11}\Gamma^1{}_{12}\right) + \left(\Gamma^2{}_{11}\Gamma^2{}_{22} - \Gamma^2{}_{21}\Gamma^2{}_{12}\right) + \left(\Gamma^2{}_{11}\Gamma^3{}_{32} - \Gamma^2{}_{31}\Gamma^3{}_{12}\right) + \left(\Gamma^2{}_{11}\Gamma^4{}_{42} - \Gamma^2{}_{41}\Gamma^4{}_{12}\right) \\ + \left(\Gamma^3{}_{11}\Gamma^1{}_{13} - \Gamma^3{}_{11}\Gamma^1{}_{13}\right) + \left(\Gamma^3{}_{11}\Gamma^2{}_{23} - \Gamma^3{}_{21}\Gamma^2{}_{13}\right) + \left(\Gamma^3{}_{11}\Gamma^3{}_{33} - \Gamma^3{}_{31}\Gamma^3{}_{13}\right) + \left(\Gamma^3{}_{11}\Gamma^4{}_{43} - \Gamma^3{}_{41}\Gamma^4{}_{13}\right) \\ + \left(\Gamma^4{}_{11}\Gamma^1{}_{14} - \Gamma^4{}_{11}\Gamma^1{}_{14}\right) + \left(\Gamma^4{}_{11}\Gamma^2{}_{24} - \Gamma^4{}_{21}\Gamma^2{}_{14}\right) + \left(\Gamma^4{}_{11}\Gamma^3{}_{34} - \Gamma^4{}_{31}\Gamma^3{}_{14}\right) + \left(\Gamma^4{}_{11}\Gamma^4{}_{44} - \Gamma^4{}_{41}\Gamma^4{}_{14}\right) \end{bmatrix}$$

$$R_{11} = \partial_4\Gamma^4{}_{11} + \begin{bmatrix} \left(\boxed{\Gamma^1{}_{11}\Gamma^1{}_{11} - \Gamma^1{}_{11}\Gamma^1{}_{11}}\right) + \left(\boxed{\Gamma^1{}_{11}}\Gamma^2{}_{21} - \boxed{\Gamma^1{}_{21}}\Gamma^2{}_{11}\right) + \left(\boxed{\Gamma^1{}_{11}}\Gamma^3{}_{31} - \boxed{\Gamma^1{}_{31}}\Gamma^3{}_{11}\right) + \left(\boxed{\Gamma^1{}_{11}}\Gamma^4{}_{41} - \Gamma^1{}_{41}\Gamma^4{}_{11}\right) \\ + \left(\boxed{\Gamma^2{}_{11}\Gamma^1{}_{12} - \Gamma^2{}_{11}\Gamma^1{}_{12}}\right) + \left(\boxed{\Gamma^2{}_{11}}\Gamma^2{}_{22} - \boxed{\Gamma^2{}_{21}}\Gamma^2{}_{12}\right) + \left(\boxed{\Gamma^2{}_{11}}\Gamma^3{}_{32} - \boxed{\Gamma^2{}_{31}}\Gamma^3{}_{12}\right) + \left(\boxed{\Gamma^2{}_{11}}\Gamma^4{}_{42} - \boxed{\Gamma^2{}_{41}}\Gamma^4{}_{12}\right) \\ + \left(\boxed{\Gamma^3{}_{11}\Gamma^1{}_{13} - \Gamma^3{}_{11}\Gamma^1{}_{13}}\right) + \left(\boxed{\Gamma^3{}_{11}}\Gamma^2{}_{23} - \boxed{\Gamma^3{}_{21}}\Gamma^2{}_{13}\right) + \left(\boxed{\Gamma^3{}_{11}}\Gamma^3{}_{33} - \boxed{\Gamma^3{}_{31}}\Gamma^3{}_{13}\right) + \left(\boxed{\Gamma^3{}_{11}}\Gamma^4{}_{43} - \boxed{\Gamma^3{}_{41}}\Gamma^4{}_{13}\right) \\ + \left(\boxed{\Gamma^4{}_{11}\Gamma^1{}_{14} - \Gamma^4{}_{11}\Gamma^1{}_{14}}\right) + \left(\Gamma^4{}_{11}\Gamma^2{}_{24} - \boxed{\Gamma^4{}_{21}}\Gamma^2{}_{14}\right) + \left(\Gamma^4{}_{11}\Gamma^3{}_{34} - \boxed{\Gamma^4{}_{31}}\Gamma^3{}_{14}\right) + \left(\Gamma^4{}_{11}\Gamma^4{}_{44} - \boxed{\Gamma^4{}_{41}}\Gamma^4{}_{14}\right) \end{bmatrix}$$

$$R_{11} = \partial_4\Gamma^4{}_{11} + \left[\left(-\Gamma^1{}_{41}\Gamma^4{}_{11}\right) + \left(\Gamma^4{}_{11}\Gamma^2{}_{24}\right) + \left(\Gamma^4{}_{11}\Gamma^3{}_{34}\right) + \left(\Gamma^4{}_{11}\Gamma^4{}_{44}\right)\right]$$

$$R_{11} = \partial_4\left(\frac{1}{2}\partial_4 \ln\psi(x_4)\right) + \left[-\left(\frac{1}{2}\partial_4 \ln\psi(x_4)\right)^2 + \left(\frac{1}{2}\partial_4 \ln\psi(x_4)\right)^2 + \left(\frac{1}{2}\partial_4 \ln\psi(x_4)\right)^2 + \left(\frac{1}{2}\partial_4 \ln\psi(x_4)\right)^2\right]$$

$$\boxed{R_{11} = \frac{1}{2}\partial_4{}^2 \ln\psi(x_4) + \frac{1}{2}\left(\partial_4 \ln\psi(x_4)\right)^2}$$

$$\boxed{R_{22} = \partial_4\Gamma^4{}_{22} + \Gamma^{\eta}{}_{22}\Gamma^{\mu}{}_{\mu\eta} - \Gamma^{\eta}{}_{\mu 2}\Gamma^{\mu}{}_{2\eta}}$$

$$R_{22} = \partial_4\Gamma^4{}_{22} + \Gamma^{\eta}{}_{22}\Gamma^{\mu}{}_{\mu\eta} - \Gamma^{\eta}{}_{\mu 2}\Gamma^{\mu}{}_{2\eta}$$

$$\boxed{R_{22} = \frac{1}{2}\partial_4{}^2 \ln\psi(x_4) + \frac{1}{2}\left(\partial_4 \ln\psi(x_4)\right)^2}$$

$$\boxed{R_{33} = \partial_4\Gamma^4{}_{33} + \Gamma^{\eta}{}_{33}\Gamma^{\mu}{}_{\mu\eta} - \Gamma^{\eta}{}_{\mu 3}\Gamma^{\mu}{}_{3\eta}}$$

$$R_{33} = \partial_4\Gamma^4{}_{33} + \Gamma^{\eta}{}_{33}\Gamma^{\mu}{}_{\mu\eta} - \Gamma^{\eta}{}_{\mu 3}\Gamma^{\mu}{}_{3\eta}$$

$$\boxed{R_{33} = \frac{1}{2}\partial_4{}^2 \ln\psi(x_4) + \frac{1}{2}\left(\partial_4 \ln\psi(x_4)\right)^2}$$

$$\left(\Gamma^1{}_{14} = \Gamma^1{}_{41}\right) = \left(\Gamma^2{}_{24} = \Gamma^2{}_{42}\right) = \left(\Gamma^3{}_{34} = \Gamma^3{}_{43}\right) = \left(\Gamma^4{}_{11} = \Gamma^4{}_{22} = \Gamma^4{}_{33} = \Gamma^4{}_{44}\right) = \frac{1}{2}\partial_4 \ln\psi(x_4)$$

$$\boxed{R_{44} = \boxed{\partial_1\Gamma^1{}_{11} + \partial_2\Gamma^2{}_{11} + \partial_3\Gamma^3{}_{11}} + \partial_4\Gamma^4{}_{11} - \partial_4\Gamma^{\mu}{}_{\mu 4} + \Gamma^{\eta}{}_{44}\Gamma^{\mu}{}_{\mu\eta} - \Gamma^{\eta}{}_{\mu 4}\Gamma^{\mu}{}_{4\eta}}$$

$$R_{44} = \partial_4\Gamma^4{}_{44} - \left[\partial_4\Gamma^1{}_{14} + \partial_4\Gamma^2{}_{24} + \partial_4\Gamma^3{}_{34} + \partial_4\Gamma^4{}_{44}\right] + \begin{bmatrix} \left(\Gamma^1{}_{44}\Gamma^1{}_{11} - \Gamma^1{}_{14}\Gamma^1{}_{41}\right) + \left(\Gamma^1{}_{44}\Gamma^2{}_{21} - \Gamma^1{}_{24}\Gamma^2{}_{41}\right) + \left(\Gamma^1{}_{44}\Gamma^3{}_{31} - \Gamma^1{}_{34}\Gamma^3{}_{41}\right) + \left(\Gamma^1{}_{44}\Gamma^4{}_{41} - \Gamma^1{}_{44}\Gamma^4{}_{41}\right) \\ + \left(\Gamma^2{}_{44}\Gamma^1{}_{12} - \Gamma^2{}_{14}\Gamma^1{}_{42}\right) + \left(\Gamma^2{}_{44}\Gamma^2{}_{22} - \Gamma^2{}_{24}\Gamma^2{}_{42}\right) + \left(\Gamma^2{}_{44}\Gamma^3{}_{32} - \Gamma^2{}_{34}\Gamma^3{}_{42}\right) + \left(\Gamma^2{}_{44}\Gamma^4{}_{42} - \Gamma^2{}_{44}\Gamma^4{}_{42}\right) \\ + \left(\Gamma^3{}_{44}\Gamma^1{}_{13} - \Gamma^3{}_{14}\Gamma^1{}_{43}\right) + \left(\Gamma^3{}_{44}\Gamma^2{}_{23} - \Gamma^3{}_{24}\Gamma^2{}_{43}\right) + \left(\Gamma^3{}_{44}\Gamma^3{}_{33} - \Gamma^3{}_{34}\Gamma^3{}_{43}\right) + \left(\Gamma^3{}_{44}\Gamma^4{}_{43} - \Gamma^3{}_{44}\Gamma^4{}_{43}\right) \\ + \left(\Gamma^4{}_{44}\Gamma^1{}_{14} - \Gamma^4{}_{14}\Gamma^1{}_{44}\right) + \left(\Gamma^4{}_{44}\Gamma^2{}_{24} - \Gamma^4{}_{24}\Gamma^2{}_{44}\right) + \left(\Gamma^4{}_{44}\Gamma^3{}_{34} - \Gamma^4{}_{34}\Gamma^3{}_{44}\right) + \left(\Gamma^4{}_{44}\Gamma^4{}_{44} - \Gamma^4{}_{44}\Gamma^4{}_{44}\right) \end{bmatrix}$$

$$R_{44} = \partial_4\Gamma^4{}_{44} - \left[\partial_4\Gamma^1{}_{14} + \partial_4\Gamma^2{}_{24} + \partial_4\Gamma^3{}_{34} + \partial_4\Gamma^4{}_{44}\right] + \begin{bmatrix} \left(\boxed{\Gamma^1{}_{44}}\Gamma^1{}_{11} - \boxed{\Gamma^1{}_{14}}\Gamma^1{}_{41}\right) + \left(\boxed{\Gamma^1{}_{44}}\Gamma^2{}_{21} - \boxed{\Gamma^1{}_{24}}\Gamma^2{}_{41}\right) + \left(\boxed{\Gamma^1{}_{44}}\Gamma^3{}_{31} - \boxed{\Gamma^1{}_{34}}\Gamma^3{}_{41}\right) + \left(\boxed{\Gamma^1{}_{44}}\Gamma^4{}_{41} - \boxed{\Gamma^1{}_{44}}\Gamma^4{}_{41}\right) \\ + \left(\boxed{\Gamma^2{}_{44}}\Gamma^1{}_{12} - \boxed{\Gamma^2{}_{14}}\Gamma^1{}_{42}\right) + \left(\boxed{\Gamma^2{}_{44}}\Gamma^2{}_{22} - \Gamma^2{}_{24}\Gamma^2{}_{42}\right) + \left(\boxed{\Gamma^2{}_{44}}\Gamma^3{}_{32} - \boxed{\Gamma^2{}_{34}}\Gamma^3{}_{42}\right) + \left(\boxed{\Gamma^2{}_{44}}\Gamma^4{}_{42} - \boxed{\Gamma^2{}_{44}}\Gamma^4{}_{42}\right) \\ + \left(\boxed{\Gamma^3{}_{44}}\Gamma^1{}_{13} - \boxed{\Gamma^3{}_{14}}\Gamma^1{}_{43}\right) + \left(\boxed{\Gamma^3{}_{44}}\Gamma^2{}_{23} - \boxed{\Gamma^3{}_{24}}\Gamma^2{}_{43}\right) + \left(\boxed{\Gamma^3{}_{44}}\Gamma^3{}_{33} - \Gamma^3{}_{34}\Gamma^3{}_{43}\right) + \left(\boxed{\Gamma^3{}_{44}}\Gamma^4{}_{43} - \boxed{\Gamma^3{}_{44}}\Gamma^4{}_{43}\right) \\ + \left(\Gamma^4{}_{44}\Gamma^1{}_{14} - \boxed{\Gamma^4{}_{14}}\Gamma^1{}_{44}\right) + \left(\Gamma^4{}_{44}\Gamma^2{}_{24} - \boxed{\Gamma^4{}_{24}}\Gamma^2{}_{44}\right) + \left(\Gamma^4{}_{44}\Gamma^3{}_{34} - \boxed{\Gamma^4{}_{34}}\Gamma^3{}_{44}\right) + \left(\boxed{\Gamma^4{}_{44}\Gamma^4{}_{44} - \Gamma^4{}_{44}\Gamma^4{}_{44}}\right) \end{bmatrix}$$

$$R_{44} = -\left[\partial_4\Gamma^1{}_{14} + \partial_4\Gamma^2{}_{24} + \partial_4\Gamma^3{}_{34}\right] + \left[\left(-\Gamma^1{}_{14}\Gamma^1{}_{41}\right) + \left(-\Gamma^2{}_{24}\Gamma^2{}_{42}\right) + \left(-\Gamma^3{}_{34}\Gamma^3{}_{43}\right) + \left(\Gamma^4{}_{44}\Gamma^1{}_{14}\right) + \left(\Gamma^4{}_{44}\Gamma^2{}_{24}\right) + \left(\Gamma^4{}_{44}\Gamma^3{}_{34}\right)\right]$$

$$R_{44} = -\frac{3}{2}\partial_4{}^2 \ln\psi(x_4) + \begin{bmatrix} -\left(\frac{1}{2}\partial_4 \ln\psi(x_4)\right)^2 - \left(\frac{1}{2}\partial_4 \ln\psi(x_4)\right)^2 - \left(\frac{1}{2}\partial_4 \ln\psi(x_4)\right)^2 \\ + \left(\frac{1}{2}\partial_4 \ln\psi(x_4)\right)^2 + \left(\frac{1}{2}\partial_4 \ln\psi(x_4)\right)^2 + \left(\frac{1}{2}\partial_4 \ln\psi(x_4)\right)^2 \end{bmatrix} \rightarrow \boxed{R_{44} = -\frac{3}{2}\partial_4{}^2 \ln\psi(x_4)}$$

$$\boxed{R_{11} = R_{22} = R_{33} = \frac{1}{2}\partial_4{}^2 \ln\psi(x_4) + \frac{1}{2}\left(\partial_4 \ln\psi(x_4)\right)^2 \ , \ R_{44} = -\frac{3}{2}\partial_4{}^2 \ln\psi(x_4)}$$

Appendix D

$$R_{11} - \frac{1}{2} R g_{11} = \kappa p$$
$$R_{11} - \frac{1}{2} R \psi(x_4) \eta_{11} = \kappa p$$
$$\frac{1}{2} {\partial_4}^2 \ln \psi(x_4) + \frac{1}{2} \left(\partial_4 \ln \psi(x_4) \right)^2 \; - \frac{1}{2} \left(3 {\partial_4}^2 \ln \psi(x_4) + \frac{3}{2} \left(\partial_4 \ln \psi(x_4) \right)^2 \right) \psi^{-1}(x_4) \psi(x_4) \eta_{11} = \kappa p$$
$$\boxed{-{\partial_4}^2 \ln \psi(x_4) \; - \frac{1}{4} \left(\partial_4 \ln \psi(x_4) \right)^2 = \kappa p}$$

$$R_{44} - \frac{1}{2} R g_{44} = \kappa \left(\varepsilon_p + \varepsilon_s \right)$$
$$R_{44} - \frac{1}{2} R \psi(x_4) \eta_{44} = \kappa \left(\varepsilon_p + \varepsilon_s \right)$$
$$-\frac{3}{2} {\partial_4}^2 \ln \psi(x_4) - \frac{1}{2} \left(3 {\partial_4}^2 \ln \psi(x_4) + \frac{3}{2} \left(\partial_4 \ln \psi(x_4) \right)^2 \right) \psi^{-1}(x_4) \psi(x_4) \eta_{44} = \kappa \left(\varepsilon_p + \varepsilon_s \right)$$
$$\boxed{\frac{3}{4} \left(\partial_4 \ln \psi(x_4) \right)^2 = \kappa \left(\varepsilon_p + \varepsilon_s \right)}$$

Appendix E

E3 - space

$$\left. \begin{array}{l} \partial_1 g_{\mu\nu}\left(x_4\right) = 0 \\ \partial_2 g_{\mu\nu}\left(x_4\right) = 0 \\ \partial_3 g_{\mu\nu}\left(x_4\right) = 0 \end{array} \right\} \rightarrow R_{\lambda\nu} = \partial_\mu \Gamma^\mu{}_{\nu\lambda} - \partial_\nu \Gamma^\mu{}_{\mu\lambda} + \Gamma^\eta{}_{\nu\lambda} \Gamma^\mu{}_{\mu\eta} - \Gamma^\eta{}_{\mu\lambda} \Gamma^\mu{}_{\nu\eta} = 0 \rightarrow \boxed{R = 0}$$

Appendix F

$$g_{\mu\nu} = \psi(x_4) \eta_{\mu\nu}$$
$$g^{\mu\nu} = \psi^{-1}(x_4) \eta^{\mu\nu}$$
$$R_{11} = R_{22} = R_{33} = \frac{1}{2} {\partial_4}^2 \ln \psi(x_4) + \frac{1}{2} \left(\partial_4 \ln \psi(x_4) \right)^2 \; ,$$
$$R_{44} = -\frac{3}{2} {\partial_4}^2 \ln \psi(x_4)$$
$$R = R_{\mu\nu} g^{\mu\nu} = R_{\mu\nu} \eta^{\mu\nu} \psi^{-1}(x_4) = \left(R_{11} + R_{22} + R_{33} - R_{44} \right) \psi^{-1}(x_4) = \left(3 {\partial_4}^2 \ln \psi(x_4) + \frac{3}{2} \left(\partial_4 \ln \psi(x_4) \right)^2 \right) \psi^{-1}(x_4)$$
$$R = \left(3 {\partial_4}^2 \ln \psi(x_4) + \frac{3}{2} \left(\partial_4 \ln \psi(x_4) \right)^2 \right) \psi^{-1}(x_4) \; \left\{ \begin{array}{l} \\ \psi_\pm(x_4) = e^{\left[\pm x_4 \sqrt{\frac{4}{3} \kappa \left(\varepsilon_p + \varepsilon_s \right)} \right]} \geq 0 \end{array} \right\} \left\{ \begin{array}{l} R = \left(\underbrace{3 {\partial_4}^2 \ln \left(e^{\left[\pm x_4 \sqrt{\frac{4}{3} \kappa \left(\varepsilon_p + \varepsilon_s \right)} \right]} \right)}_{0} + \frac{3}{2} \left(\partial_4 \ln \left(e^{\left[\pm x_4 \sqrt{\frac{4}{3} \kappa \left(\varepsilon_p + \varepsilon_s \right)} \right]} \right) \right)^2 \right) {\psi_\pm}^{-1}(x_4) \\ \boxed{R\left(\psi_\pm(x_4) \right) = 2 \kappa \left(\varepsilon_p + \varepsilon_s \right) {\psi_\pm}^{-1}(x_4) \geq 0} \end{array} \right\}$$

References

1. Zwicky, F. On the Redshift of Spectral Lines Through Interstellar Space. *Proc. Natl. Acad. Sci. USA* **1929**, *15*, 773–779. [CrossRef] [PubMed]
2. Bondi, H.; Gold, T. The Steady-State Theory of the Expanding Universe. *Mon. Not. R. Astron. Soc.* **1948**, *108*, 252–270. [CrossRef]
3. Hoyle, F. A New Model for the Expanding Universe. *Mon. Not. R. Astron. Soc.* **1948**, *108*, 372–382. [CrossRef]
4. Bekenstein, J.D. Exact solutions of Einstein-conformal scalar equations. *Ann. Phys. N. Y.* **1974**, *82*, 535–547. [CrossRef]
5. Lester, J.A. Conformal Minkowski space-time—I—Relative infinity and proper time. *Nuovo Cim. B* **1982**, *72*, 261–272. [CrossRef]
6. Lester, J.A. Conformal Minkowski spacetime—II—A Cosmological model. *Nuovo Cim. B* **1983**, *73*, 139–149. [CrossRef]
7. Varieschi, G.U. A kinematical approach to conformal cosmology. *Gen. Relativ. Gravit.* **2010**, *42*, 929–974. [CrossRef]
8. Behnke, D.; Blaschke, D.B.; Pervushin, V.N.; Proskurin, D. Description of supernova data in conformal cosmology without cosmological constant. *Phys. Lett. Sect. B Nucl. Elem. Part High-Energy Phys.* **2002**, *530*, 20–26. [CrossRef]
9. Libanov, M.; Rubakov, V.; Rubtsov, G. Towards conformal cosmology. *JETP Lett.* **2015**, *102*, 561–570. [CrossRef]
10. Kumar, M.M. Some significant conformal metrics. *Nuovo Cim. A Ser.* **1969**, *63*, 559–573. [CrossRef]
11. Lematre, A.G. A Homogeneous Universe of Constant Mass and Increasing Radius accounting for the Radial Velocity of Extra-galactic Nebulae. *Mon. Not. R. Astron. Soc.* **1931**, *91*, 483–490. [CrossRef]

12. Friedmann, A. On the Possibility of a World with Constant Negative Curvature of Space. *Gen. Relativ. Gravit.* **1999**, *31*, 2001–2008. [CrossRef]
13. Robertson, H.P. Kinematics and World-Structure. *Astrophys. J.* **1935**, *82*, 284. [CrossRef]
14. Walker, A.G. On Milne's Theory of World-Structure. *Proc. Lond. Math. Soc.* **1937**, *S2–S42*, 90–127. [CrossRef]
15. Weinberg, S. *Relativity, Gravitation and Cosmology*; John Wiley & Sons Inc.: Hoboken, NJ, USA, 1972.
16. Ibison, M. On the conformal forms of the Robertson-Walker metric. *J. Math. Phys.* **2007**, *48*, 122501. [CrossRef]
17. Misner, C.W.; Thorne, K.S.; Wheeler, J.A. MTW-Gravitation. In *Gravitation*; W. H. Freeman and Company: New York, NY, USA, 2018.
18. Peebles, P.J. *Principles of Physical Cosmology*; Princeton University Press: Princeton, NJ, USA, 2020. [CrossRef]
19. Kuchař, K. *Fundamentals of General Relativity*; ACADEMIA: Prahy, Czech Republic, 1968.
20. Weinberg, S. *Cosmology*; Oxford Press: Oxford, UK, 2008.
21. NASA. NASA/IPAC Extragalactic Database (2022): Date and Time of the Query: Sun Nov 12 09:25:30 2017PDT. Available online: https://ned.ipac.caltech.edu/ (accessed on 1 March 2023).
22. Planck 2013. Planck 2013 Results: I. Overview of Products and Scientific Results, Astronomy & Astrophysics Manuscript no. Planck Mission. Available online: https://arxiv.org/pdf/1303.5062.pdf (accessed on 1 March 2023).
23. Mitra, A. Interpretational conflicts between the static and non-static forms of the de Sitter metric. *Sci. Rep.* **2012**, *2*, 923. [CrossRef] [PubMed]
24. Schmidt, M.; Higdon, J.C.; Hueter, G. Application of the V/V (max) test to gamma-ray bursts. *Astrophys. J.* **1988**, *329*, L85–L87. [CrossRef]
25. Band, D.L. The effect of repeating burst sources on $\langle V/V \text{ max} \rangle$. *AIP Conf. Proc.* **1994**, *307*, 39–43. [CrossRef]
26. Meegan, C.A.; Fishman, G.J.; Wilson, R.B.; Paciesas, W.S.; Pendleton, G.N.; Horack, J.M.; Brock, M.N.; Kouveliotou, C. Spatial distribution of γ-ray bursts observed by BATSE. *Nature* **1992**, *355*, 143–145. [CrossRef]
27. NASA. Gamma-Ray Astrophysics: NSSTC, BATSE4B, CMAXMIN Table. Available online: https://gammaray.nsstc.nasa.gov/batse/grb/catalog/4b/4br_cmax_cmin.html (accessed on 1 March 2023).
28. Salafia, O.S.; Ghirlanda, G. The Structure of Gamma Ray Burst Jets. *Galaxies* **2022**, *10*, 93. [CrossRef]
29. Sciama, D.W.; Rees, M.J. Cosmological significance of the relation between red-shift and flux density for quasars. *Nature* **1966**, *211*, 1283. [CrossRef]
30. MILLIQUAS v7.9. MILLIQUAS v7.9: Quasars, Redshifts and the 'Accelerating-Expansion' Universe. Data, Sky Fields, & Some Thoughts on the Right Cosmological Model. Available online: https://quasars.org/milliquas.htm (accessed on 6 January 2025).
31. Halpern, P.; Tomasello, N. Size of the Observable Universe. *Adv. Astrophys.* **2016**, *1*, 135–137. [CrossRef]
32. Finkelstein, S.L.; Bagley, M.B.; Haro, P.A.; Dickinson, M.; Ferguson, H.C.; Kartaltepe, J.S.; Papovich, C.; Burgarella, D.; Kocevski, D.D.; Huertas-Company, M.; et al. A Long Time Ago in a Galaxy Far, Far Away: A Candidate z∼12 Galaxy in Early JWST CEERS Imaging. *Astrophys. J. Lett.* **2022**, *940*, L55. [CrossRef]